Canadian Mineralogist
Vol. 26, pp. 603-625 (1988)

MINERALOGY AND GEOCHEMISTRY OF A HYDROTHERMAL SILICA–SULFIDE–SULFATE SPIRE IN THE CALDERA OF AXIAL SEAMOUNT, JUAN DE FUCA RIDGE

MARK D. HANNINGTON AND STEVEN D. SCOTT

Marine Geology Research Group, Department of Geology, University of Toronto, Toronto, Ontario M5S 1A1

ABSTRACT

Axial Seamount is a large shield volcano on the central Juan de Fuca Ridge, northeastern Pacific Ocean. A 21-km^2 summit caldera is host to low-temperature (<35°C) hydrothermal vents and large, chimney-like spires near its northern wall. Hydrothermal activity is closely associated with recently active eruptive fissures. An intact spire (160 kg) recovered from the caldera is comprised of amorphous silica, sphalerite, marcasite, barite, wurtzite, chalcopyrite, and galena, with trace amounts of pyrite, jordanite, Pb–As–Sb–Ag sulfosalts, tetrahedrite–tennantite, native sulfur, and Fe and Mn oxides. The bulk chemical composition of the spire is: 28.5% SiO_2, 22.7% Zn, 8.7% Ba, 5.8% Fe, 0.43% Cu, 0.35% Pb, and 18.6% S, with 570 ppm As, 350 ppm Sb, 186 ppm Ag, 4.9 ppm Au, 522 ppm Cd, 1470 ppm Sr, and 600 ppm Mn. Au is conspicuously high at concentrations up to 6.7 ppm. Mineral paragenesis in the spire is related to changes in temperature, the degree of seawater mixing, and pH–aS_2–aO_2 conditions during its growth. Constraints on the temperature of formation were determined from amorphous silica solubility in sampled vent fluids (<235°C), fluid inclusions in wurtzite (up to 250°C), and published equilibrium $\delta^{18}O$ values for barite–water (185°C). The $\delta^{34}S$ values for $BaSO_4$ (+16.1 to +21.2 ‰), FeS_2 (+1.1 to +3.9 ‰), and ZnS (+4.2 to + 5.7‰) indicate isotopic disequilibrium among these phases and suggest local reduction of sulfate from seawater at the site of deposition. The complex multistage history of the spire reflects growth at temperatures of <300°C during mixing between higher temperature fluids and seawater. This process is important for the accumulation of sulfides at many seafloor vent sites and in their ancient analogs on land.

Keywords: seafloor polymetallic sulfides, Axial Seamount, Juan de Fuca Ridge, mineralogy, chemical composition, mineral chemistry, fluid inclusions, sulfur isotopes.

SOMMAIRE

Le guyot de Axial est un puissant édifice volcanique en bouclier situé dans la partie centrale de la dorsale de Juan de Fuca, dans le nord-est de l'océan Pacifique. Une caldéra de 21 km^2 à son sommet est le site d'évents hydrothermaux de basse température (<35°C) et d'édifices en forme de cheminée près de la paroi nord. L'activité hydrothermale est localisée le long de fissures éruptives récemment actives. Une cheminée intacte (160 kg), découverte dans la caldéra, contient: silice amorphe, sphalérite, marcasite, baryte, wurtzite, chalcopyrite et galène, avec traces de pyrite, jordanite, sulfosels de Pb–As–Sb–Ag, tétraédrite–tennantite, soufre natif, et oxydes de Fe et de Mn. La cheminée a la composition chimique globale suivante (%, en poids): SiO_2 28.5, Zn 22.7, Ba 8.7, Fe 5.8, Cu 0.43, Pb 0.35, et S 18.6, et contient les éléments traces (teneurs en ppm): As 570, Sb 350, Ag 186, Au 4.9, Cd 522, Sr 1470, et Mn 600. La teneur en or est anormalement élevée, puisqu'elle atteint un maximum de 6.7 ppm. La séquence de cristallisation dépend de la température, du degré de mélange avec l'eau de mer, et des conditions de pH, de aS_2 et de aO_2 pendant la croissance de l'édifice. La température de formation a été déterminée à partir de la solubilité de la silice amorphe dans les fluides des évents (<235°C), des inclusions fluides dans la wurtzite (jusqu'à 250°C), et des valeurs publiées du partage de $\delta^{18}O$ entre baryte et phase aqueuse (185°C). Les valeurs de $\delta^{34}S$ pour la baryte (entre +16.1 et +21.2‰), FeS_2 (entre +1.1 et +3.9‰), et ZnS (entre +4.2 et +5.7‰) témoignent d'un déséquilibre isotopique parmi ces phases, qui serait dû à une réduction locale de sulfate dans l'eau de mer au site de déposition. L'évolution polyphasée complexe de la cheminée résulte de sa croissance à des températures inférieures à 300°C au cours du mélange entre fluides de température plus élevée et l'eau de mer. C'est un processus important pour l'accumulation des sulfures, aussi bien au site des évents actuels sur les fonds marins que sur terre, dans leurs analogues anciens.

(Traduit par la Rédaction)

Mots-clés: sulfures polymétalliques marins, guyot de Axial, dorsale de Juan de Fuca, minéralogie, composition chimique, chimie des minéraux, inclusions fluides, isotopes de soufre.

INTRODUCTION

In 1983, hydrothermal vent fields and a small sulfide deposit were discovered in the caldera of Axial Seamount on the central Juan de Fuca Ridge (Fig. 1: 45°57′N, 130°02′W) using the Canadian deep-diving submersible, PISCES IV (CASM II 1985, Scott 1985). A small sulfide deposit discovered in the northwest corner of the caldera (Fig. 2) consists of three large chimney-like structures, standing 4–10 m in height, and a number of smaller structures capping a buried sulfide mound of unknown size. Although hydrothermal activity in the area is only weak at present, this study provides evidence for the former existence of high-temperature vents.

According to recent models for the accumulation of massive sulfides on the seafloor, large deposits are grown from small, high-temperature (>300°C) vents or black smokers through sustained hydrothermal activity (*e.g.*, Hékinian *et al.* 1985, Hékinian & Fouquet 1985, Tivey & Delaney 1986). Vent fields like those at 21°N on the East Pacific Rise (Haymon & Kastner 1981, Goldfarb *et al.* 1983) are charac-

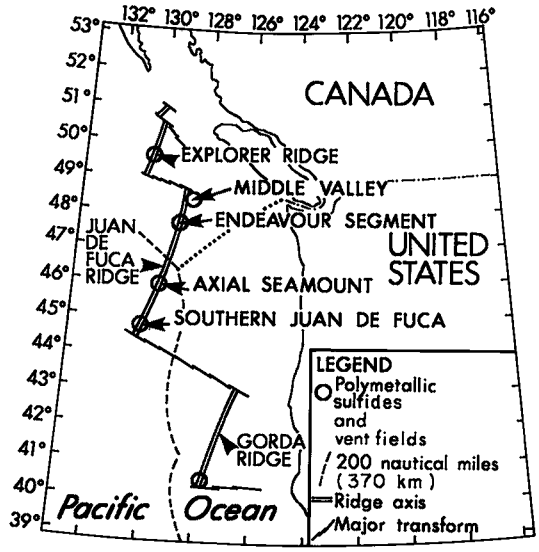

FIG. 1. Location of seafloor polymetallic sulfide deposits in the northeastern Pacific.

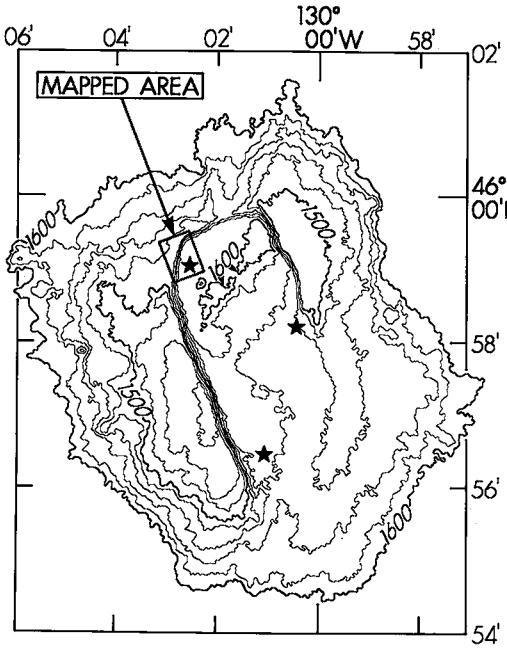

FIG. 2. SEABEAM bathymetry of the Axial Seamount caldera (from CASM II 1985). Vent fields (stars) occur within the study area and at the southern end of the caldera (Malahoff *et al.* 1984, ASHES Expedition 1986). The 1500 m and 1600 m isobaths are labelled; the contour interval is 20 m.

terized by a predominance of small (<5 m in height) active chimneys with relatively few large mounds and are referred to as "immature". In contrast, "mature" deposits like those at Southern Explorer Ridge (Scott *et al.* 1984, 1985, CASM III 1985) are characterized by abundant broad-based structures known as spires, which coalesce to form large sulfide mounds tens of meters in diameter. Individual spires grow as a result of sustained mineral precipitation at a single vent and can reach heights of more than 10 m. Collectively, the sulfide mounds grown from these spires form deposits of several million tonnes (*e.g.*, Scott *et al.* 1988, Rona *et al.* 1986).

Black smokers alone cannot account for the efficient accumulation of sulfides at hydrothermal vents. More than 90% of the metals from a typical black smoker are lost to diffuse hydrothermal plumes as buoyant solutions escape to the water column (Converse *et al.* 1984, Edmond *et al.* 1982). Therefore, the growth of large sulfide spires is an important means of trapping hydrothermal fluids and may be critical for the local accumulation of hydrothermal precipitates. Although fragments of sulfide chimneys have been identified in ancient deposits (Scott 1981, Oudin & Constantinou 1984), few intact spires are preserved because of their tendency to become incorporated in hydrothermally reworked mounds. Consequently, little is known about this aspect of the formation of massive sulfide deposits. To investigate the growth of large sulfide-bearing structures, we have examined a 160-kg, intact spire recovered from Axial Seamount during CASM II (1985).

The sampled spire formed at relatively low temperatures (<300°C) and is mineralogically and geochemically distinct from the small, high-temperature chimneys studied by Goldfarb *et al.* (1983) and Haymon (1983). Similar structures may have been responsible for the accumulation of low-temperature (<300°C) sulfides and sulfates on top of many ancient massive sulfide deposits. We briefly compare the physical and chemical conditions of mineralization at Axial Seamount with those of other deposits on the seafloor to show that the hydrothermal fluids responsible for the growth of large spires at Axial Seamount may have been derived from high-temperature solutions (up to 350°C) by a combination of conductive cooling and mixing with local seawater.

GEOLOGY AND HYDROTHERMAL ACTIVITY IN THE CALDERA OF AXIAL SEAMOUNT

Axial seamount is a large shield volcano, 50 km by 70 km at its base (2600 m deep), with a 3 km by 7 km summit caldera (minimum depth of 1490 m). Active spreading along the axis of the central Juan de Fuca Ridge intersects the caldera obliquely and is expressed by abundant north–south-trending fissures in its northern wall. The caldera is a vertical-

walled structure with a nearly flat floor (<5 m of relief), bounded by fault offsets that are 60 to 80 m in height. The southern wall of the caldera is breached and covered by sheet flows (Fig. 2).

An eruptive fissure in the floor of the caldera extends southward from the northwest wall for 300 m (Fig. 3). The fissure consists of seven overlapping collapse-structures cut by a central cleft (CASM II 1985). Sheet flows, pock-marked by drained and collapsed lava ponds, cover most of the caldera floor; fresh pillow and lobate lavas occur along the fissure. Drain-back features in the fissure (*i.e.*, collapsed lava and draped lava on the fissure walls) indicate that it is the source of recent lava flows. This suggestion is substantiated by the sparse cover of pelagic sediment (<5–10% by area) near the eruptive fissure compared to the thick cover of sediment outside the caldera walls.

Three hydrothermally active areas have been located within the caldera of Axial Seamount (Fig. 2). The first, at the northern end of the caldera, includes a number of warm-water vents occupying three of the collapsed structures in the eruptive fissure. The vents occur at open fractures in basalt on the bottom of the fissure or along its walls. Several vents are inhabited by pogonophoran tube worms in mound-like colonies up to 2 m in diameter (Fig. 4a; CASM II 1985). Hydrothermal fluids emanating from the fractures are less than 35°C (ambient seawater 1.5 to 2°C). A partly buried sulfide deposit occurs 40–50 m to the east, along a narrow, north–south-trending fracture zone about 30 m in length (Fig. 3). This fracture zone is interpreted to be an older eruptive fissure covered by recent sheet flows. A second hydrothermal site, at the southern end of the caldera (Fig. 2), consists of vents at temperatures up to 330°C, sulfide edifices, and Fe oxide deposits (Malahoff *et al.* 1984, ASHES Expedition 1986). A third, low-temperature (<300°C) vent site was discovered by the ASHES Expedition (1986) near the eastern wall of the caldera.

Hydrothermal fluids at Axial Seamount are focused along the faults bounding the caldera and at the intersection of these faults with the spreading center of the Juan de Fuca Ridge. Similar volcano-tectonic settings have focused the flow of fluids in ancient massive sulfide-forming environments (*e.g.*, Cathles 1983, Ohmoto & Takahashi 1983). Fractures and eruptive fissures around the margins and within calderas have been recognized as a control on the localization of the Kuroko deposits in Japan (Ohmoto 1978, Scott 1978, 1980). The eruptive fissures that characterize post-caldera volcanism and active spreading of the ridge crest at Axial Seamount provide channelways for hydrothermal solutions. Frequent eruptions of lava in the caldera create the necessary contrasts in permeability required to focus

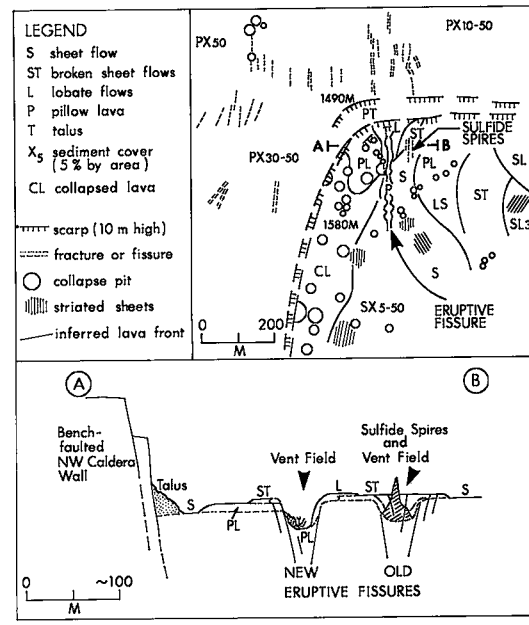

FIG. 3. Simplified geologic map of the study area showing the outline of the caldera wall, eruptive fissure, distribution of principal lava morphologies, and location of the sulfide deposit. (A–B) is a schematic cross-section through the eruptive fissure and the partly buried sulfides. The 160-kg spire was recovered from this deposit.

ascending fluids.

The presence of a large, sustained, high-level magma chamber at the summit of Axial Seamount is suggested by the large size of the volcano (1750 km^3), its vast caldera, and the abundant volcanic and tectonic activity. Most other seamounts along spreading ridges in the Eastern Pacific are small by comparison (<100 km^3) and are considered to be part of the normal magmatic budget of the ridges (Batiza 1982). Axial Seamount, however, represents an excess of volcanism on the Juan de Fuca Ridge. This combination of excess volcanic activity, a high-level magma chamber, and a highly permeable caldera, provides an opportunity for protracted hydrothermal activity. The advective heat-loss over the strike length of the Axial Seamount caldera (113 megawatts/km: Crane *et al.* 1984) is comparable to that of the vent field at 21°N, East Pacific Rise (EPR) (140 megawatts/km: Macdonald *et al.* 1980), even though the spreading rate at Axial Seamount (3 cm/yr half-rate) is only half that of the EPR.

THE GROWTH OF SULFIDE STRUCTURES AT SEAFLOOR HYDROTHERMAL VENTS

The Axial Seamount spire

The 160-kg spire described in this paper (Fig. 5)

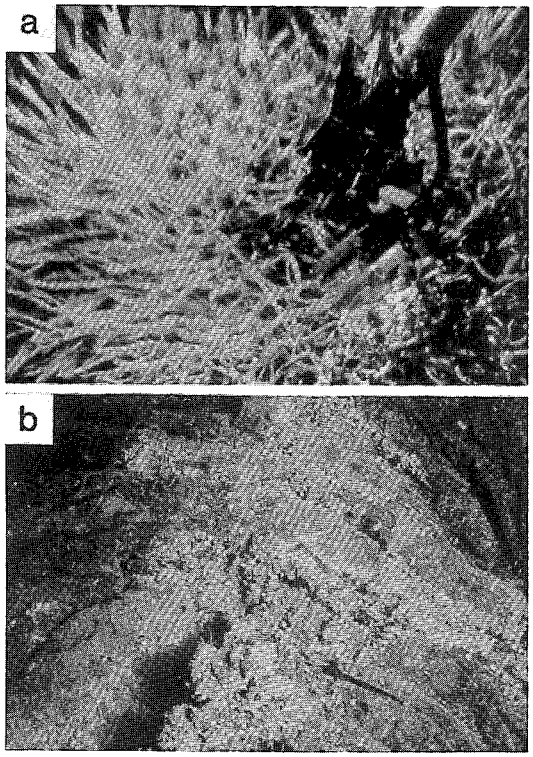

FIG. 4. Bottom photographs, taken by CASM II (1985), of active vents in the study area. a) Sampling of hydrothermal fluid venting through a colony of tube worms in the eruptive fissure. The field of view is 1 m across. b) Venting of hydrothermal fluid through a fracture in fresh basaltic lava near the sulfide deposit. The field of view is 3–4 m across.

was sampled from the small sulfide deposit in the northern vent field. Three large spires make up the bulk of the exposed sulfides in the deposit and amount to approximately 20,000 kg. By analogy with other seafloor deposits, these spires likely sit atop a larger sulfide mound that has been buried by recent lava flows. The sulfides from this deposit resemble samples from the low-temperature (<300°C) caps of large, mature mounds at Southern Explorer Ridge (Scott *et al.* 1984, 1985, CASM III 1985, Hannington *et al.* 1986).

Vents (<50°C) at open fractures in the basalt (Fig. 4b) occur in close proximity to the sulfide deposit. The coexistence of these small, low-temperature vents and the large sulfide spires grown from earlier, higher-temperature chimneys attests to the sustained nature of local hydrothermal activity. One of the large spires was 4 m in height and 2 m in diameter; it still vented warm water (19°C) and was populated by a dense biological colony. The two adjacent spires were 6 to 10 m in height, but had no major biological colonies. The existence of hydrothermal fluid in the porous interiors of these spires was indicated by cracks in their outer walls which leaked vent fluids and were lined by filamentous bacteria. The 160-kg spire was recovered near the base of one of these larger structures, and venting of warm water occurred at this site after the spire was sampled.

The spire is composed primarily of Zn and Fe sulfides, amorphous silica, and barite. Its growth history has been reconstructed from a study of the morphology and mineralogy of the structure through five cross-sections, including examination of 45 polished thin sections.

Growth of the spire began within a colony of tube worms, similar to those which inhabit vents in the nearby eruptive fissure (Fig. 4a). The worm tubes were fossilized by the early precipitation of barite and silica and formed the broad, porous substrate on which the spire was constructed. Fossilized remnants of similar worm tubes have been found in Cretaceous massive sulfides of the Semail ophiolite in Oman (Haymon *et al.* 1984) and the Troodos ophiolite in Cyprus (Oudin 1983).

Within the protective framework of silica, barite, and fossilized worm tubes, Zn and Fe sulfides were precipitated in response to steep thermal and chemical gradients between the hydrothermal fluid and surrounding seawater. Unlike black-smoker chimneys, the spire lacks a well-defined central orifice (Fig. 5); sulfides were deposited in a porous network of interconnecting channelways. Silica and barite accumulated at the top of the spire (Fig. 6a) and eventually sealed off these channelways, forcing the hydrothermal fluids to circulate within the porous interior. Trapped fluids periodically escaped through the walls or at the base of the spire, giving rise to new chimneys on its flanks, together with sulfide protrusions at the former sites of venting (Fig. 6b). At least four accretionary zones making up the spire are outlined by fossil sulfate walls and worm tubes in its interior (Fig. 7). Sulfide- and silica-lined cavities in the core of the spire are the unfilled fluid conduits.

Sulfide structures at other deposits

Typical black-smoker chimneys (*e.g.*, on the EPR at 21°N and 13°N) are maintained at high temperatures (>300°C) and therefore contain little silica and are virtually barite-free (Haymon & Kastner 1981, Hékinian & Fouquet 1985). These chimneys are initially cemented by anhydrite which is progressively replaced by sulfides through interaction with high-temperature fluids, or simply dissolved in cold seawater as a result of its retrograde solubility (Haymon 1983). In addition, the fossilized worm tubes found in large spires are not abundant in the sulfides from black smokers. In the absence of a stable silica or barite cement and a suitable biological substrate, black smokers characteristically form small,

narrow chimneys less than 1–5 m in height which are inherently unstable and ultimately crumble (*e.g.*, Haymon & Kastner 1981).

Amorphous silica is responsible for the lasting stability of some large sulfide structures found on the Endeavor Ridge (Tivey & Delaney 1986). Silica was precipitated in these structures by conductive cooling of the saturated solutions. The growth and stability of large spires at Southern Explorer Ridge, like those at Axial Seamount, is predicated on the availability of abundant barite as well as silica. Barite was precipitated from Ba in the vent fluids upon mixing with sulfate-rich seawater. The abundance of barite depends largely on the amount of Ba leached from the source rocks by the hydrothermal fluids. Barium is efficiently extracted from basalts during circulation of seawater (Seyfried & Bischoff 1981, Seyfried & Mottl 1982) so its concentration in the vent fluids is controlled by the composition of the underlying rocks. At Southern Explorer Ridge and Axial Seamount, the basalts are enriched in Ba by almost an order of magnitude over normal EPR MORB (Cousens *et al.* 1984, R.L. Chase, pers. comm. 1986). These enriched basalts may account for the high barite content of the deposits and the abundance of large sulfide spires compared to vent sites on the EPR and elsewhere on the Juan de Fuca Ridge. In a similar manner, the sediments underlying deposits in the Guaymas Basin, Gulf of California, provide abundant calcite for the construction of large sulfide-bearing structures up to 20 m in height (Peter 1986, Peter & Scott 1988, Scott 1985).

After a phase of venting at temperatures up to 350°C, substantial cooling of the hydrothermal fluid by a combination of conduction and mixing with SO_4-rich seawater is required for the precipitation of amorphous silica and barite. Deposition of these minerals at temperatures <300°C may be necessary in order to form the large spires commonly found on top of mature deposits. The growth of these structures has been observed at temperatures as low as 150°C (Johnson & Tunnicliffe 1985, 1986). However, there is compelling evidence for continued high-temperature mineralization, beneath the protective cap of low-temperature spires, from fluids trapped within large, mature mounds. Vents on top of sulfide mounds at Southern Explorer Ridge locally discharge fluids at temperatures up to 306°C, while nearby spires on the same mound vent much cooler fluids at <100°C (SCHISM I 1984, Tunnicliffe *et al.* 1986). This suggests that individual vents at different temperatures on a single mound are fed by the same high-temperature fluid at depth. Local mixing with seawater near the surface of the mounds results in low-temperature discharge and accounts for the growth of large, low-temperature spires accompanying higher temperature mineralization at the same site. By analogy with ancient deposits, the sulfide mounds are likely reworked by contemporaneous hydrothermal fluids beneath the low-temperature sulfides and sulfates, resulting in well-known mineralogical zonations common to massive sulfides on land (*e.g.* Eldridge *et al.* 1983). At 13°N on the EPR, Hékinian *et al.* (1985) and Hékinian & Fouquet (1985) have described zoned sulfide deposits where high-temperature (320–350°C) sulfides have formed

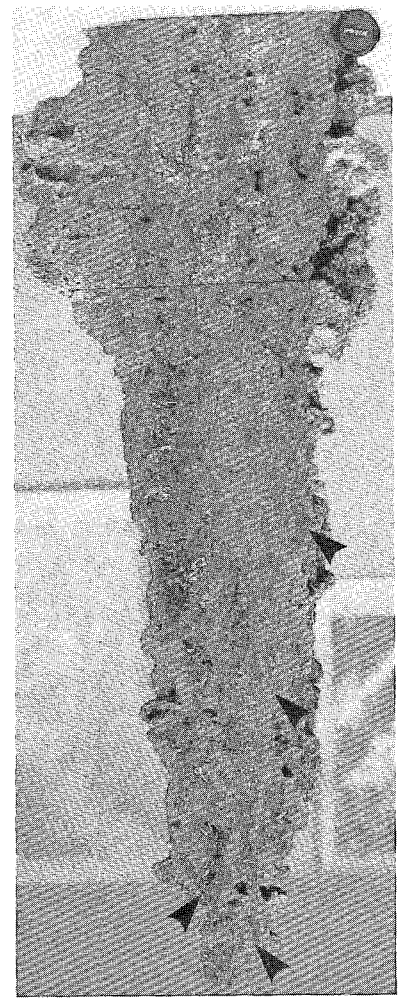

FIG. 5. Vertical cross-section of the spire from Axial Seamount showing its complex internal morphology. A thick rind of sulfate- and silica-cemented worm tubes (white) encloses porous Zn-rich sulfides (black) in the core of the spire. Silica and sulfate cap the spire (see also Fig. 6a). White salt from seawater outlines porous zones in the Zn sulfides. Large, silica-filled cavities mark the fluid channels, and sulfate-rich walls in the interior of the spire outline former zones of accretion (arrows). Lens cap at lower left is 6 cm in diameter.

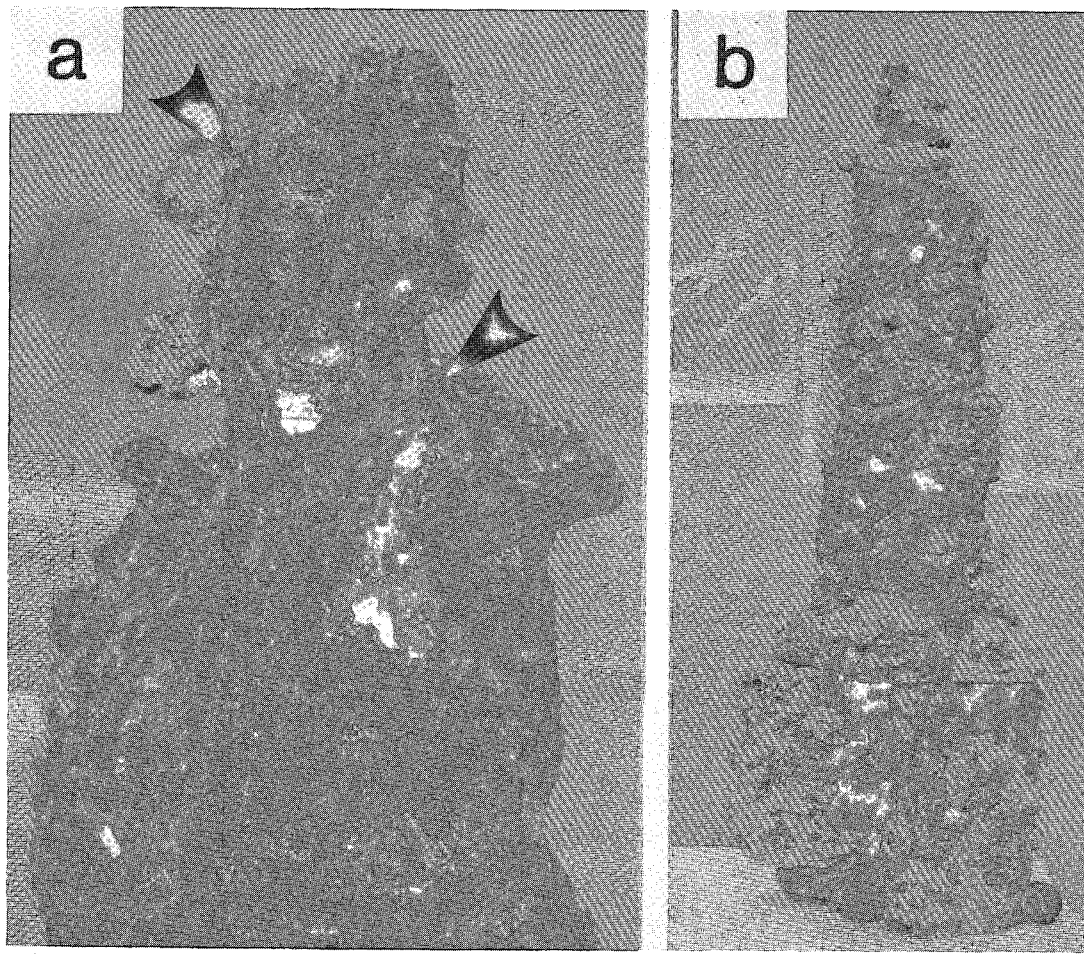

FIG. 6. The top of the spire (a) is capped by barite and amorphous silica. Two fluid channels (arrows) are outlined by sulfate-rich walls and are filled by Zn sulfides. The exterior of the spire (b) is coated by dark Fe and Mn oxides. The broad base is composed of barite and silica that replaced a fossil tube-worm colony. Lens cap at lower left is 6 cm across.

beneath low-temperature (<200°C) mineralization. This wide range of temperatures in most deposits causes complex patterns of mineralization, dissolution, and recrystallization.

MINERALOGY AND PARAGENESIS

The mineralogy and paragenesis of the Axial Seamount spire (Fig. 8) can be summarized as: (1) early, low-temperature, barite–silica deposition in the sulfate-rich walls of the spire (Fig. 9a); (2) main-stage, higher temperature sulfide deposition in the porous interior (Fig. 9b,c); and (3) late-stage silicification throughout the spire (Fig. 9d). The overall mineralogy is typical of that described for white-smoker chimneys at 21°N (Oudin 1981, 1983, Haymon & Kastner 1981). Most of the precipitates are fine-grained (<1 mm), but some crystals of wurtzite and barite, which line open cavities, reach 5 mm in length. These coarse, euhedral crystals are most common in the porous core of the spire.

Silica and fibrous barite comprise the early framework-building assemblage (Fig. 10a) and form the walls of the spire on which later main-stage sulfides were precipitated. Worm tubes are initially mantled by silica and barite (Fig. 10a) and may be replaced by later sulfides (Fig. 10b). Traces of anhydrite occur in samples from the large active spire (19°C), but anhydrite is absent in the others.

Fine-grained particles of marcasite and sphalerite ($\leq 1\mu$m) are disseminated throughout early amorphous silica in the barite–silica stage. Coarser mar-

casite and sphalerite occur within and mantling early, fibrous barite (Fig. 10c). Intergrown Fe sulfides and barite indicate that both reduced and oxidized sulfur were available at the time of deposition. Barite from the barite–silica stage is commonly replaced by later massive amorphous silica (Figs. 9d, 10c).

Amorphous silica throughout the spire forms homogenous, colloform layers up to 1 mm thick or loosely packed aggregates of uniform silica spheres, 1 to 10 μm across (Fig. 10d). Similar material in low-temperature vents at 21°N has been described as opal (Oudin 1981), but the silica from Axial Seamount shows a single, broad X-ray peak characteristic of an amorphous, noncrystalline phase (Jones & Segnit 1971, Kano & Taguchi 1982). Bacterial precipitation of delicate silica "strings" has also been documented in samples from Axial Seamount (Juniper & Fouquet 1988).

Framboidal marcasite is the earliest important sulfide and consists of spheroidal aggregates of individual Fe-sulfide particles up to 0.1 μm in diameter (Fig. 10e). Later main-stage marcasite, in the core of the spire, consists of banded spherules (5 to 10 μm in diameter) and massive colloform aggregates which have locally recrystallized (Fig. 10f). Although the cores of some marcasite framboids have inverted to pyrite, pyrite is generally scarce in the spire. An amorphous Fe–S–SiO_2 phase (Fig. 11a) is locally intergrown with the framboidal and colloform marcasite; an energy-dispersion microprobe analysis gives a composition of 60% Fe, 20% S, and 20% SiO_2 by weight.

Marcasite in other seafloor deposits occurs primarily in association with siliceous, Zn-rich sulfides at <300°C (Picot & Fevrier 1980, Oudin 1981, 1983, Kingston *et al.* 1983, Hékinian & Fouquet 1985). At 21°N, marcasite is abundant only in white smokers and in inactive chimneys and mounds (Oudin 1981, 1983, Haymon & Kastner 1981).

Zn sulfides constitute nearly 80% of the sulfides in the spire. The main stage of sulfide deposition includes: (1) massive aggregates of sphalerite (Fig. 11b) with chalcopyrite, galena and tetrahedrite–tennantite; (2) later colloform and banded sphalerite (Fig. 11c); and (3) cavity-lining wurtzite (Fig. 11d). Sphalerite in massive aggregates is opaque and Fe-rich compared to later colloform varieties. The colloform sphalerite commonly possesses light, Fe-poor rims with darker, Fe-rich cores (Fig. 11c). Chalcopyrite and galena occur as epitactic growths on sphalerite grains; no significant replacement of sphalerite by chalcopyrite (*i.e.*, "chalcopyrite disease") is observed in polished section. Dendritic galena locally occurs in the core zone of late-stage sphalerite blebs (Fig. 11c).

Wurtzite crystals form tapered hexagonal prisms, typically 0.05–2 mm in length (Fig. 11d). They commonly have dark, Fe-rich cores and lighter, Fe-poor rims, but are generally less Fe-rich than the earlier sphalerite. Estimates of the relative abundance of the two polymorphs based on petrography and X-ray-diffraction scans of sulfide concentrates indicate that wurtzite accounts for about 30% of the Zn sulfides. Whereas sphalerite occurs throughout the spire, euhedral crystals of wurtzite occur only in open cavities. At 21°N and the Southern Juan de Fuca Ridge, wurtzite is also found in the cores of active chimneys (Haymon & Kastner 1981, Oudin 1981, 1983, Koski *et al.* 1984); sphalerite occurs in both active and inactive chimneys, but dominates the inactive spires and mounds (Hékinian *et al.* 1980, Picot & Fevrier 1980, Zierenberg *et al.* 1984).

Late-stage hydrothermal fluids were rich in Pb, As, Sb, Ag and Au. Galena partly mantles colloform sphalerite and is commonly overgrown by, or altered to, jordanite (Fig. 11e). Two additional Pb–As–Sb–

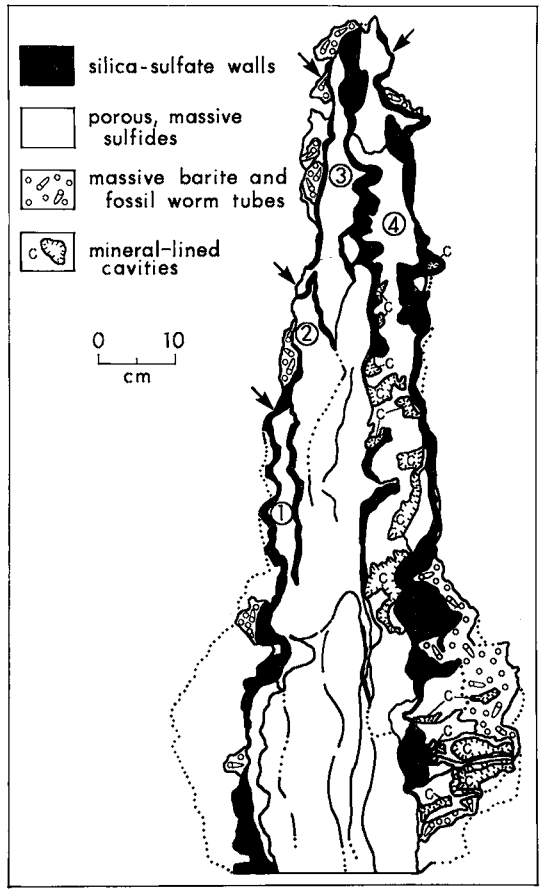

FIG. 7. Four accreted growth zones in the spire (circled numbers) are outlined by sulfate- and silica-rich zones and fossilized worm tubes. Venting of hydrothermal fluid occurred at the top of each accreted zone (arrows).

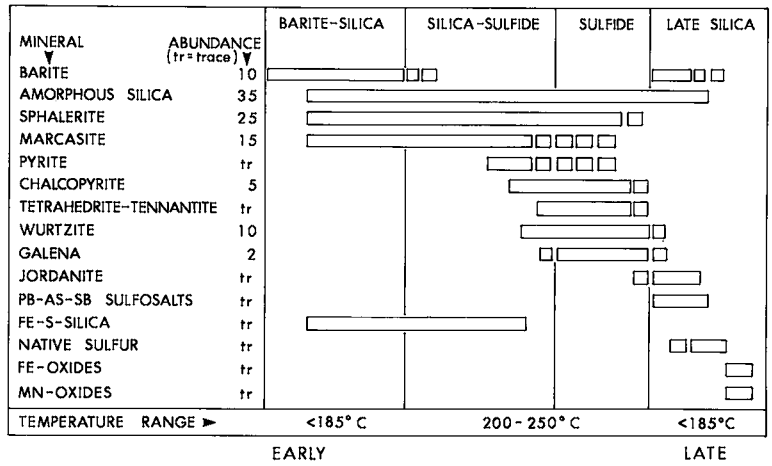

FIG. 8. Mineral paragenesis in the spire. Solid bars represent the distribution of major minerals from early to late stages; broken bars are minor occurrences. Average mineral abundances are given in volume percent. Temperature estimates for the different stages of mineralization are discussed in the text.

Ag sulfosalts are associated with jordanite as fine, sinter-like disseminations (Fig. 11f). Up to 6.7 ppm Au occurs with this sulfosalt assemblage, probably as finely divided free gold or gold–silver alloy (Hannington *et al.* 1986). Native sulfur locally is present with late-stage amorphous silica in the core of the spire and may have been derived from oxidation of excess H_2S in the late hydrothermal fluids. Clots of barite crystals which line some of the cavities indicate that seawater-diluted fluids continued to circulate through the spire after the main stage of sulfide mineralization.

An outline of the thermal history of the spire, corresponding to the paragenetic sequence (Fig. 8), was determined from the geothermometry of local vent fluids and specific mineral phases as discussed in detail below. Increasing temperatures (up to about 250°C) from the early deposition of barite and silica to the main stage of sulfide mineralization correspond to a decrease in the amount of mixing between high-temperature fluids and cold ambient seawater during the growth of the spire.

ANALYTICAL METHODS

Mineral analyses were obtained by energy dispersion on an ETEC automated microprobe and a JEOL scanning electron microscope interfaced with an X-ray microanalyzer. Details of analytical procedures and standards are provided by Hannington (1986).

Concentrations of major and trace elements in samples from the spire were determined by X-ray Assay Laboratories, Don Mills, Ontario, and by neutron activation at the Slowpoke nuclear reactor, University of Toronto. Concentrations of Fe, SiO_2, Ca, Na, K, Al, Mn, Mg, Ti and P, along with Sr, Rb, Cr, Y, Nb and Zr, were determined from fused glass discs by wavelength-dispersion X-ray fluorescence to minimum detection limits (MDL) of 0.01 wt.% and 10 ppm, respectively. Cu, Zn, Pb, S and Ba were determined by X-ray fluorescence from pressed powder pellets. As, Sb, and Bi were determined by flameless atomic absorption with a quartz tube furnace (MDL 0.1 ppm). Se and Te were determined by graphite furnace (MDL 0.1 ppm). Multielement emission spectrometry with argon plasma excitation was used for Mo, Cd, Ge, Ni and Co (MDL 1.0 ppm); a spark source was used for Sn. Ag was determined by fire assay (MDL 0.5 ppm); Au was determined by fire-assay preconcentration with an atomic absorption finish (MDL 2 ppb). CO_2 was determined by titration. Neutron activation was used for analysis of duplicate samples for Cu, Zn, Ba, Ca, Na, Al, Mn, Sr, Mg and Cl.

Homogenization temperatures of fluid inclusions were measured on a Linkham TH600 heating/freezing stage at the F.G. Smith Fluid Inclusion Laboratory, University of Toronto (Macdonald & Spooner 1981). Sulfur isotope ratios were determined at the Duncan Derry Laboratory, University of Ottawa. Mineral separates were prepared at the Geological Survey of Canada. The fine-grained nature of the precipitates necessitated chemical separations. Analytical precision based on multiple analyses of two standards is ± 1.3‰ (1 s.d.) of the reported value (G.S.C. standard: +1.9 ± 0.1 per mil; University of Calgary standard: +19.6 ± 0.3 per mil). Duplicate samples were analyzed at the U.S. Geological Survey, Reston.

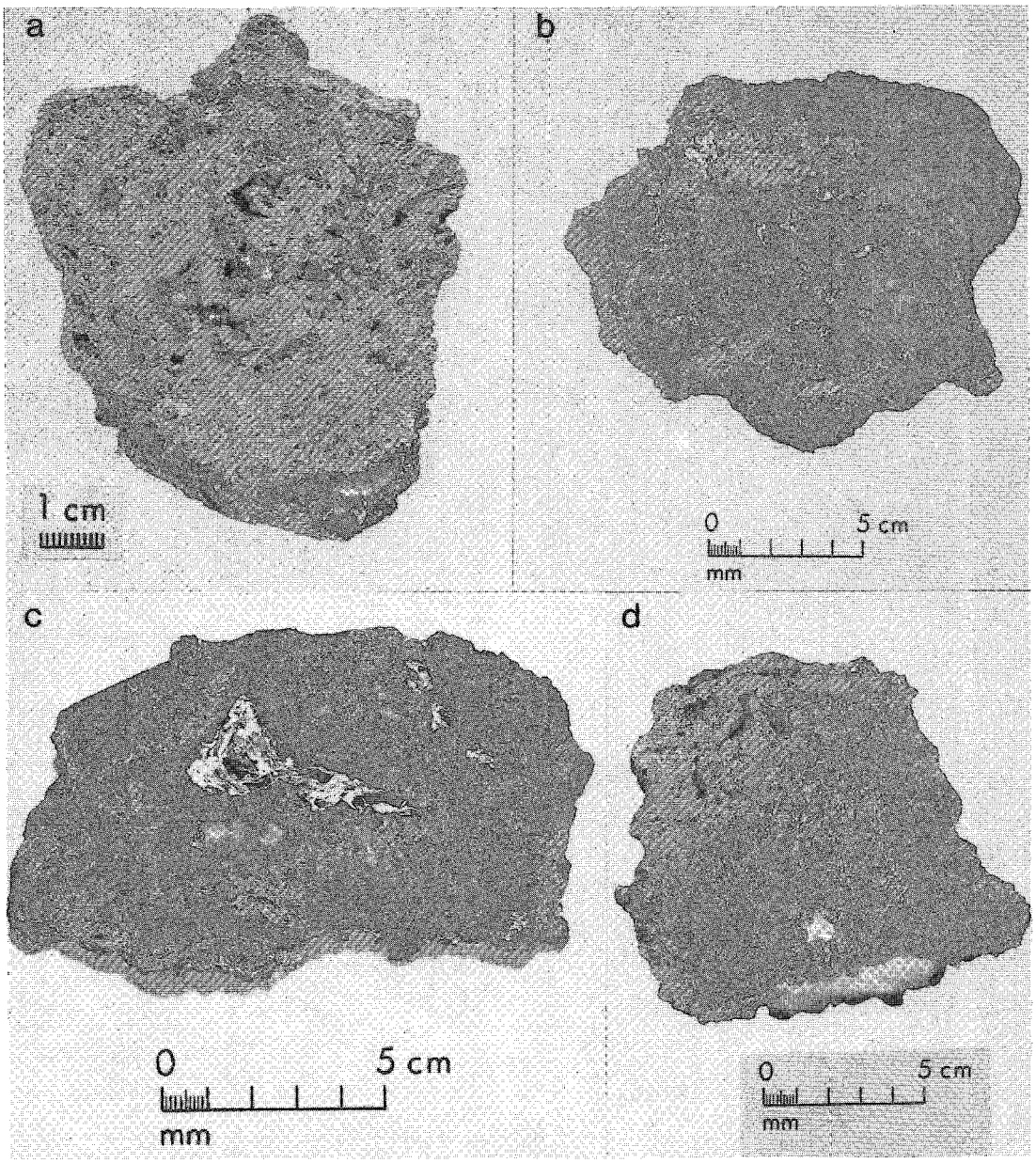

FIG. 9. a) Typical barite-rich sample from the Axial Seamount spire. Fossilized worm tubes (circular structures) and clots of barite crystals occur in the center of the sample. b) Sample from the base of the spire showing an outer silica- and sulfate-rich wall (grey) and Zn sulfide-rich core (black). Fossil worm tubes occur both in sulfides and sulfates. c) Zn sulfide-rich material from the core of the spire. The large cavity is filled with late-stage amorphous silica. d) Silicified sample, with desiccation cracks, from a large inactive spire adjacent to the 160-kg spire. Large cavities are lined by late-stage barite crystals.

MINERAL CHEMISTRY

The Fe content of sphalerite varies from <1 to 8 wt.%, with a distinct maximum in the massive, main-stage sphalerite. Up to 1 wt.% Cu is present in more than 80% of the sphalerite analyses, though visible microscopic inclusions of chalcopyrite are rare. Chalcopyrite inclusions smaller than the

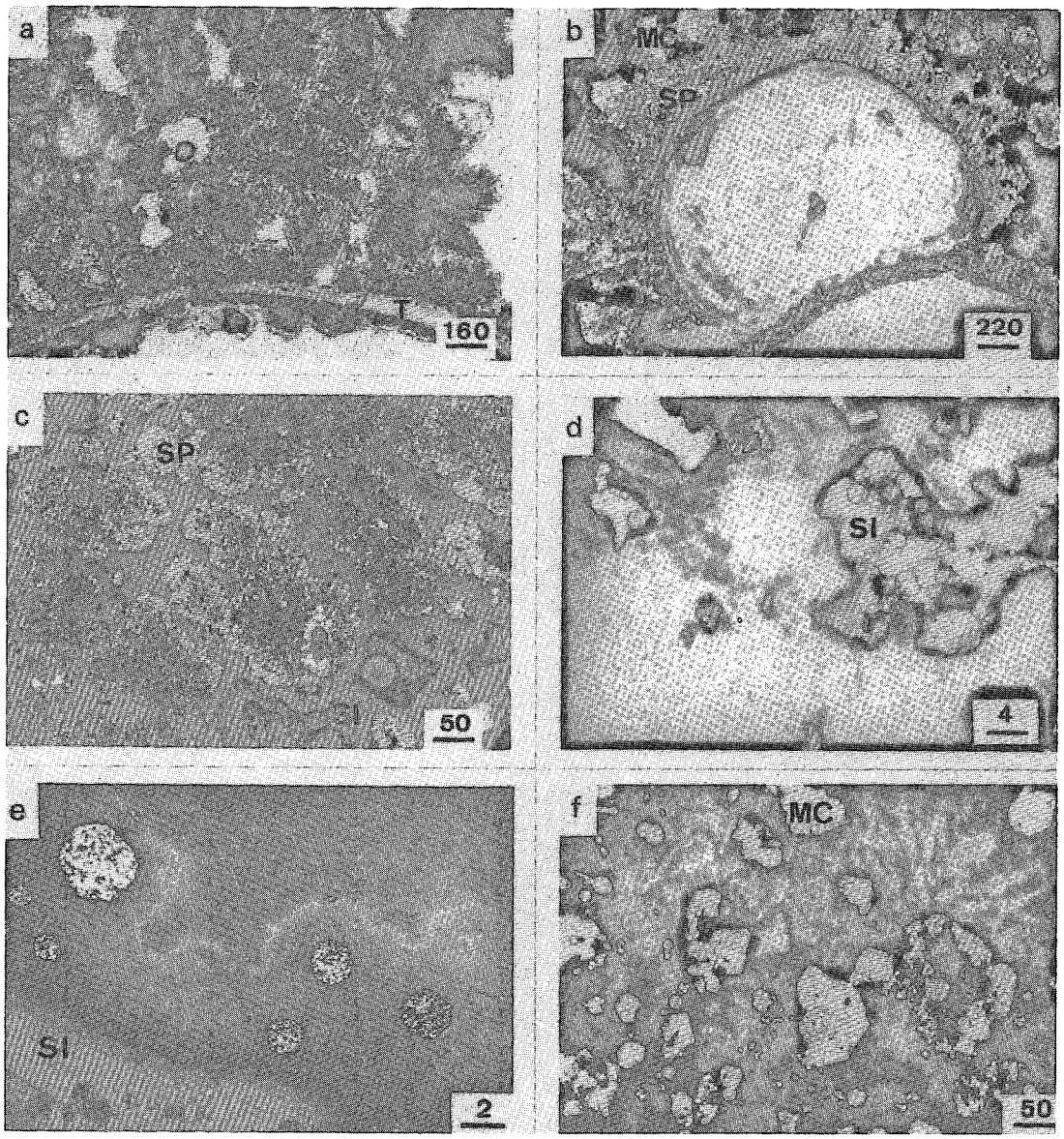

FIG. 10. Photomicrographs of typical textures in the early stages of mineralization. Scale bars are in micrometers. a) Sheath-like barite mantled by amorphous silica on a fossilized worm tube (T) (transmitted light). b) Sphalerite (SP) and marcasite (MC) that replace and mantle a worm tube (reflected light). c) Sheath-like barite replaced by amorphous silica and overgrown by sphalerite (reflected light). d) Spheres of amorphous silica (SI) in cavities between crystals of wurtzite (WZ) (transmitted light). e) Framboids of marcasite in amorphous silica (reflected light). f) Recrystallized marcasite on earlier framboids of marcasite in a matrix of amorphous silica and barite (reflected light).

microprobe beam may contribute to the measured FeS content of the sphalerite. Therefore, analyses of Cu-bearing sphalerite are corrected by subtracting an amount of Fe equal to the amount of Cu on an atomic basis (*e.g.*, Urabe 1974). Available Cu-free analyses belong to the same statistical population as the corrected analyses (99% confidence); the mean is 3.7 ± 1.3 mole % FeS (1 s.d.). About 85% of the sphalerite analyses fall in the range of 0.1 to 6 mole % FeS (Fig. 12).

The variation in the FeS content of different generations of sphalerite (Fig. 13) reflects changing con-

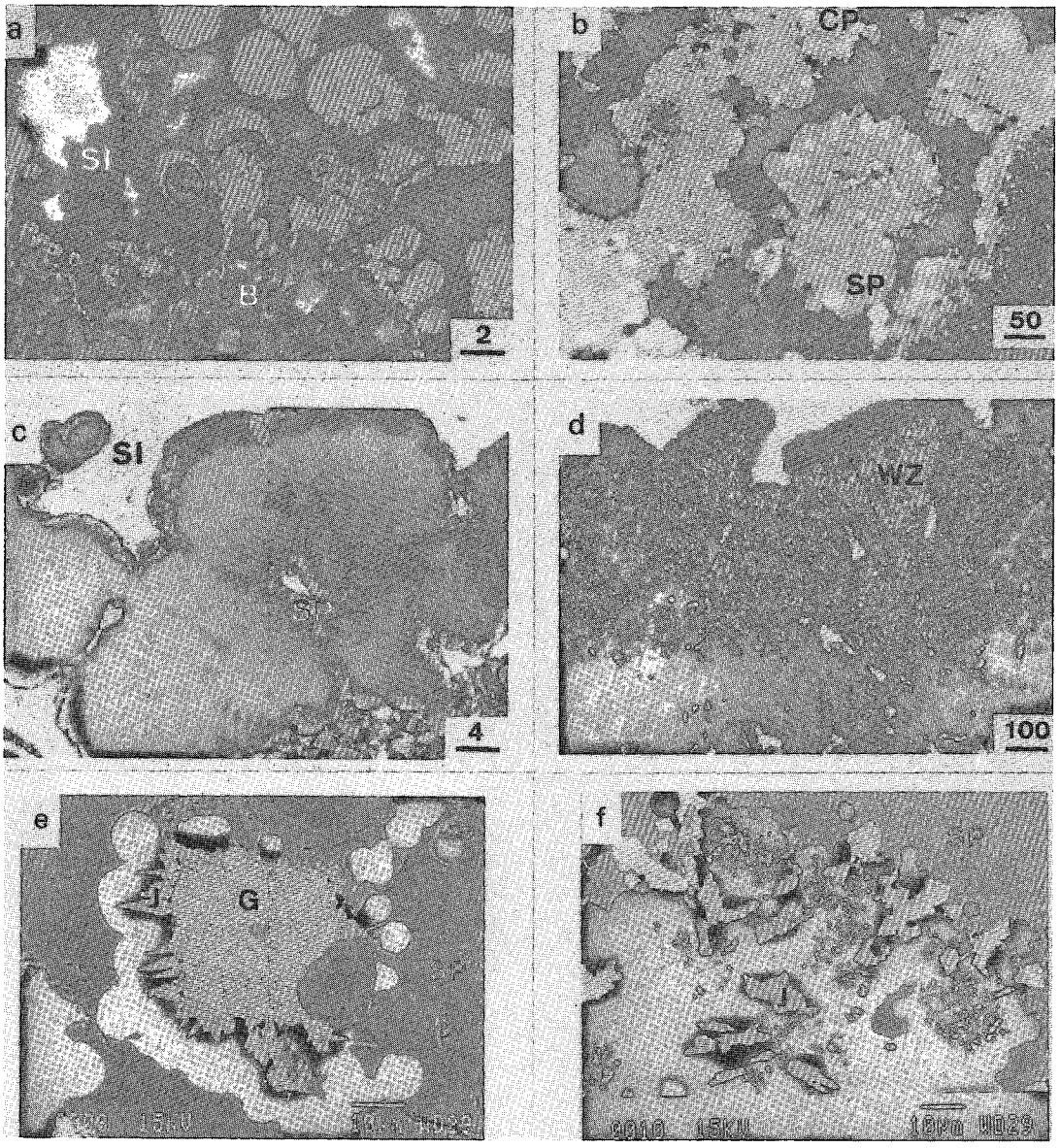

FIG. 11. Photomicrographs of typical textures in the main and late stages of mineralization. Scale bars are in micrometers. a) Amorphous Fe–S–SiO_2 phase (light grey) on coarse barite blades. The dark matrix is amorphous silica (reflected light). b) Granular aggregates of sphalerite with epitactic inclusions of chalcopyrite (CP) (reflected light). c) Colloform blebs of sphalerite showing Fe-rich cores and Fe-poor rims. Dendritic galena (black) occurs within the sphalerite (transmitted light). d) Tapered crystals of wurtzite in a cavity. A thin mantle of Fe-rich sphalerite occurs at the ends of the crystals (transmitted light). e) Jordanite crystals (J) on galena (G) (backscattered electron image). Spheres of silica (black) surround the jordanite and galena. f) Jordanite grains and patches of sinter-like sulfosalts within amorphous silica (backscattered electron image).

ditions in the mineralizing fluid throughout the growth of the spire. An increase in FeS contents during the main stage of mineralization indicates increasing temperature or decreasing sulfur activity (Barton & Toulmin 1966, Czamanske 1974, Scott 1983).

Microprobe analyses of barite from the spire indi-

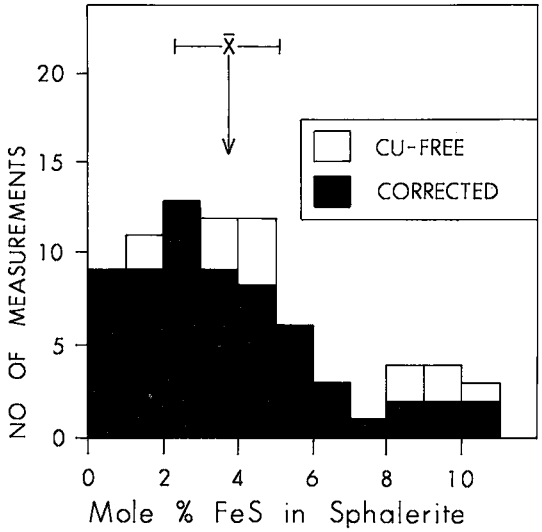

FIG. 12. Distribution of FeS contents from 72 analyses of sphalerite in the Axial Seamount spire. The mean FeS content (3.7 mole percent) is shown with one standard deviation (1.3 mole percent). Corrected values have atomic proportions of Fe = Cu subtracted from the total Fe. Corrected and Cu-free analyses belong to the same statistical population at a 99% confidence level.

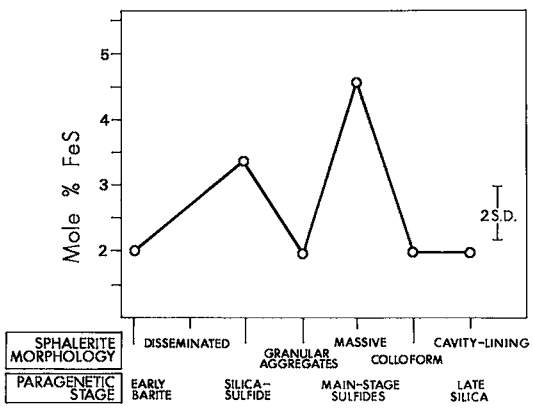

FIG. 13. Distribution of average corrected FeS contents of sphalerite from different paragenetic stages in the spire (see Fig. 8). The FeS contents are highest in the main-stage massive sphalerite.

cate an average of 0.8 wt.% Ca and 3.4 wt.% Sr in barite from the sulfate-rich zones, although bulk chemical analyses indicate much lower Sr contents in barite from the sulfide-rich zones. The Sr contents of barite reach 3.9 wt.% in the upper and outer portions of the spire, and 4.4 wt.% in the late barite crystals that line cavities in its core. Barite intergrown with sulfides contains <1 wt.% Sr. The higher Sr/Ba ratio in barite from sulfate-rich stages of mineralization (Fig. 14) may be a result of (1) fluctuations in the availability of Sr in the mineralizing fluid, (2) temperature-dependent partition coefficients [K_D(Sr)] for barite (Starke 1962) and, possibly (3) the degree of supersaturation of the fluids with respect to barite (*e.g.*, as for anhydrite: Shikazono & Holland 1983). The average Sr/Ba atomic ratios in barite are 0.006 for main-stage sulfide mineralization, 0.04 for silica–sulfide and barite–silica stages, and 0.08 for late-stage barite. For a K_D(Sr) of 0.16 at 200°C (Starke 1962), corresponding values of Sr/Ba in the precipitating fluids assuming equilibrium with the barite would have been 0.04, 0.25, and 0.50, respectively. Whereas most vent fluids have high concentrations of both Sr (10 to 15 ppm) and Ba (1 to 3 ppm) (*e.g.*, Von Damm 1983, Von Damm *et al.* 1985), seawater contains abundant Sr (7.7 ppm) but virtually no Ba. Therefore, an increase in the availability of Sr relative to Ba must have occurred when ambient seawater mixed with the vent fluid during precipitation of the early barite–silica assemblage and late, cavity-lining barite. Similar paragenetic variations in the Sr/Ba ratio and $^{87}Sr/^{86}Sr$ ratios in barite from Kuroko ores indicate that mixing between seawater and the ore-forming fluids also occurred in these deposits (Farrell 1979, Kalogeropoulos & Scott 1983, 1986, Farrell & Holland 1983).

Three sulfosalts have been identified through partial semiquantitative analyses of 13 individual grains: (1) a Cu-rich sulfosalt similar to tetrahedrite–tennantite, containing 3-4 wt.% combined As and Sb; (2) jordanite containing 10–12 wt.% As; and (3) an unidentified Pb–As–Sb–Ag sulfosalt, containing up to 10 wt.% combined As and Sb. The analyses obtained for each sulfosalt likely represent mixtures. Silver ranges from 1–3 wt.% in all three sulfosalts and is highest in the Sb-rich phases. These increase in abundance relative to As-rich phases late in the paragenesis.

BULK GEOCHEMISTRY

Results of 13 bulk chemical analyses of 50-g samples through the 160-kg spire, plus one sample from an adjacent spire (1327-2) are given in Table 1. Samples 1324-2, 2(2), and 2(3) are random samples from the 160-kg spire. A bulk sample of fossilized worm tubes from the base of the spire was also selected for analysis.

SiO_2, Zn, and Ba account for 65 wt.% of the spire. Fe averages 6 wt.%, and Cu and Pb each averages less than 1 wt.%. About 10% of the sulfur is present as sulfate. Average concentrations (wt.%) of important minor elements are: 0.15 Sr, 0.22 Ca, 0.07 Mn and 0.05 Cd. Mn occurs as Mn-oxide crusts

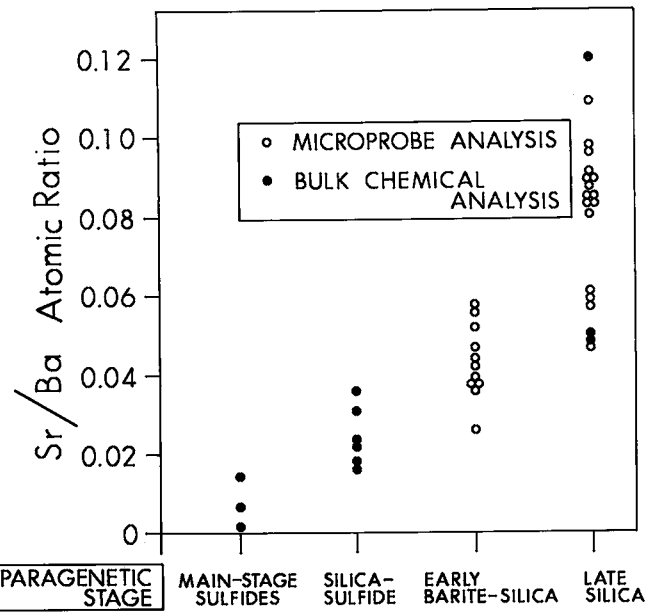

FIG. 14. Paragenetic variations in Sr/Ba atomic ratios in barite from the spire. Barite associated with sulfides is too fine-grained for accurate microprobe analysis. For these, Sr/Ba ratios were calculated from bulk chemical analyses of 50-g samples. Lower Sr/Ba ratios in barite associated with sulfides are attributed to limited mixing of seawater with the precipitating fluid.

on the exterior of the spire. The spire also contains significant average concentrations of Ag (186 ppm), Au (4.9 ppm), As (570 ppm) and Sb (350 ppm). Gold contents range from 2.9 to 6.7 ppm and are the highest yet found in unaltered sulfides on the seafloor (Hannington *et al.* 1986). Desiccated seawater salt accounts for most of the Na and Cl. Potassium, Al and Mg may be present in minute amounts of clay minerals. Fragments of basalt glass trapped in the sulfides and sulfates are common and may account for some of the remaining trace elements. Ignition of sulfur results in a high L.O.I. and high totals.

FLUID CHEMISTRY

Dilute, 29°C hydrothermal fluid from an active vent in the eruptive fissure at Axial Seamount was sampled by CASM II (McDuff *et al.* 1983). An undiluted, end-member composition can be calculated from the measured Mg content of the CASM II fluid by assuming that the unmixed high-temperature, end-member contains no Mg (Bischoff & Seyfried 1978, Edmond *et al.* 1979a). The measured composition of the CASM II fluid and its calculated end-member are given in Table 2, along with fluid compositions from several other vent sites in the eastern Pacific. The calculated end-member composition for Axial Seamount must be considered with caution because of the extent of the extrapolation. However, its similarity to measured end-member fluids at 21°N lends credence to the calculation. The measured, low-temperature fluid at Axial Seamount is strikingly similar to vent fluids at the same temperature from the Galapagos Rift.

By analogy with measured 350°C fluids at 21°N (Table 2: Von Damm 1983, Von Damm *et al.* 1985) the end-member pH of the Axial Seamount fluid is estimated to be about 3.5 to 4. The effects of mixing a 21°N-type end-member with seawater have been calculated by Janecky & Seyfried (1984). After cooling to a temperature of about 250°C and allowing for precipitation of supersaturated minerals during mixing, the 21°N fluid would have a pH near 5. The fluid at Axial Seamount is assumed to have had a similar pH at 250°C.

The low Fe content of the calculated end-member at Axial Seamount suggests losses due to subsurface precipitation, as suggested for vent fluids in the Guaymas Basin (Bowers *et al.* 1985). Although Fe is depleted in the end-member for Axial Seamount, SiO_2, Ba and Ca are similar, or enriched, relative to the fluids from other vent sites (Table 2). The total

Table 1. BULK CHEMICAL COMPOSITIONS OF SELECTED SAMPLES FROM SECTIONS OF THE RECOVERED AXIAL SEAMOUNT SPIRE AND AN ADJACENT SPIRE

Section	Exterior		Intermediate			Interior			Central	Upper	Other Samples				Fossil
Sample	SB15	SB33	SB17-18	SB41	SB20-22	SB28	SB13	SB16-17	SC51	S 53	1324-2 [1]	2(2)	2(3)	1327-2	Worm Tubes
Cu wt.%	0.09	0.43	0.44	0.78	0.57	0.48	0.75	0.34	0.61	0.12	0.12	0.50	0.09	0.29	<0.04
Fe	6.64	7.06	6.50	5.64	8.53	4.87	4.83	5.48	5.70	5.10	5.81	6.71	2.81	3.19	-
Zn	4.34	26.2	24.7	34.7	30.9	20.9	39.2	16.9	31.8	8.62	10.2	30.8	3.15	28.2	<3.0
Pb	0.55	0.28	0.44	0.10	0.25	0.44	0.11	0.54	0.23	0.19	0.63	0.59	0.44	0.13	-
S	16.0	20.4	19.8	20.8	23.0	18.6	24.8	16.7	21.7	11.3	-	20.3	12.7	-	-
SiO_2	32.0	39.4	32.7	24.6	27.0	21.3	15.5	27.9	33.5	36.5	30.2	29.0	22.7	20.4	-
Ba	18.3	6.38	5.97	0.05	0.67	3.82	0.50	2.78	7.16	23.5	14.9	1.96	34.2	14.2	34.4
Ca	0.31	0.21	0.21	0.05	0.19	0.05	0.20	0.26	0.19	0.34	0.19	0.30	0.36	0.14	0.36
Na	0.80	1.20	1.36	1.92	0.20	2.49	2.17	2.49	0.85	0.26	-	1.72	1.15	-	1.66
K	0.08	0.16	0.08	0.07	0.08	0.11	0.07	0.10	0.06	0.04	0.06	0.11	0.12	-	-
Al	0.30	1.48	0.69	0.72	0.82	1.14	0.82	0.62	0.58	0.25	0.41	0.91	0.21	-	0.05
Cl	0.21	0.10	0.11	0.12	0.12	0.22	0.27	0.23	0.16	0.10	-	0.15	0.35	-	0.44
CO_2	-	-	0.4	0.5	0.4	-	0.7	0.3	-	<0.1	0.3	-	-	0.2	-
Au ppb	6100	6100	6400	3650[2]	4500	5900	3700	5100	4500	3550[3]	-	6700	2900	-	-
Ag ppm	210	241	260	152	201	280	62.4	216	146	117	175	229	122	233	-
As	740	510	590	420	640	540	510	480	620	560	-	600	620	-	-
Sb	380	350	380	130	350	660	370	380	380	150	-	500	160	-	-
Bi	0.4	0.2	<0.1	0.1	0.9	0.2	<0.1	0.2	<0.1	0.5	-	0.3	0.4	-	-
Mo	43	36	32	32	35	53	39	30	37	49	45	37	38	32	-
Cd	60	460	540	1200	800	410	970	680	610	150	110	560	13	740	-
Ge	<10	<10	<10	30	40	10	<10	40	<10	40	-	<10	20	-	-
Se	1.8	1.1	1.6	4.5	1.9	5.0	1.9	3.5	1.8	1.4	-	2.5	1.6	-	-
Te	<0.1	<0.1	<0.1	<0.1	<0.1	<0.1	<0.1	<0.1	<0.1	<0.1	-	<0.1	<0.1	-	-
Sn	5	3	3	3	3	7	5	3	3	10	-	30	3	-	-
Mn	700	700	620	540	700	540	540	540	390	470	470	540	310	1300	1700
Co	-	-	-	-	-	-	-	-	-	-	3	-	-	3	-
Ni	-	-	-	-	-	-	-	-	-	-	32	-	-	11	-
Sr	4150	720	820	10	60	20	20	2120	720	3680	-	200	5080	-	-
Rb	<10	<10	<10	<10	<10	<10	<10	<10	<10	<10	-	10	10	-	-
Mg	360	660	240	240	480	420	1200	540	120	240	<60	540	420	-	-
Ti	<340	240	300	60	120	120	60	600	300	<270	-	300	1200	-	-
Cr	<10	10	10	20	10	20	20	<10	<10	<10	-	10	<10	-	-
P	130	40	40	40	40	40	40	40	40	90	-	90	130	-	-
Y	<10	<10	<10	<10	<10	<10	<10	<10	<10	<10	-	<10	<10	-	-
Nb	10	10	10	10	20	10	20	10	10	<10	-	<10	<10	-	-
Zr	70	<10	10	<10	<10	<10	<10	30	<10	70	-	10	80	-	-
LOI wt.%	16.8	13.8	14.4	16.4	16.3	15.1	16.5	13.8	15.6	12.0	-	15.3	9.3	-	-

1) average of two analyses. 2) average of two analyses (3600, 3700 ppb). 3) average of two anlyses (4000, 3100 ppb).

reduced sulfur content as H_2S is similar to that of measured end-member fluids from 21°N and to the inferred sulfur content of ore-forming fluids responsible for many volcanogenic massive sulfides on land (*e.g.*, 10^{-3} – 10^{-2} molal or 34 – 340 ppm H_2S for Kuroko ores: Sato 1973, Kajiwara 1973, Ohmoto & Rye 1974, Large 1977).

Elements that are quantitatively leached from basalt during interaction with hydrothermal seawater can be used to calculate approximate water/rock mass ratios, based on their net addition to the vent fluid (Von Damm 1983, Von Damm *et al.* 1985). At Axial Seamount, Ba, Li, and Rb contents in the calculated end-member fluid suggest an average water/rock mass ratio of about 2. Similar calculations and oxygen isotope data for fluids from 21°N indicate a water/rock ratio of about 0.5–0.7 (Von Damm *et al.* 1985). The small difference in the water/rock mass ratio for Axial Seamount and 21°N cannot account for the large differences in the composition of their hydrothermal precipitates. The mineralogical and chemical differences between these deposits most likely relate to the cooling and mixing histories of their hydrothermal fluids as discussed below.

GEOTHERMOMETRY

Temperatures of formation for the Axial Seamount spire are constrained by fluid inclusions, oxygen-isotope fractionation factors, and the solubility of amorphous silica. A minimum temperature for the main stage of sulfide mineralization has been determined from 67 primary and pseudosecondary, two-phase fluid inclusions in coarse wurtzite crystals in three samples from the spire (Fig. 15a). Uncorrected homogenization temperatures range from 173 to 240°C (Fig. 16). A hydrostatic confining pressure of 150 bars at Axial Seamount requires a pressure correction of +10°C. This results in a mean pressure-corrected filling temperature of 235 ± 13°C (1 s.d.) and indicates that sulfides were being deposited at temperatures at least as high as 250°C (Fig. 16). Fluid inclusions are abundant in the amorphous silica (Fig. 15b), but these invariably leaked during heating.

Shanks *et al.* (1984) measured a $\delta^{18}O$ value of +8.5 per mil in a sample of barite from the spire, and calculated a temperature of formation of about 185°C. This is consistent with paragenetic observations which suggest that barite was precipitated at lower temperatures and higher degrees of seawater mixing than the main-stage sulfides.

The temperature of the calculated end-member fluid can be estimated if the fluid is assumed to have equilibrated with quartz in the source region. A minimum temperature of about 350°C is required to ac-

TABLE 2. TYPICAL VENT FLUID COMPOSITIONS AT SOME SEAFLOOR POLYMETALLIC SULFIDE DEPOSITS

	Axial Seamount[1]		21°N, EPR[2]	Guaymas Basin[3]	Galapagos[4]	Explorer Ridge[5]		Seawater[6]
Maximum Temp.°C	29	350	355	315	30	25-85	276-306	
pH	6.18	-	3.55	5.9	6.65	6.67	4.82	7.7
H_2S ppm	11.2	224	255	167	11.2	<2	28.4	0
C	51.8	-	-	-	33	-	-	29
Cl	18860	-	18932	21591	18945	19095	18860	19093
SiO_2	66	1139	1055	694	74.4	24.2	297	9.6
SO_4	2490	0	0	0	2500	1802	1111	2672
CO_2	1760	-	250	saturated[7]	-	-	-	120
Ca	443	1146	651	2730	66-436	444	1025	406
Ba	0.18	3	1.65	4.74	0.14-0.32	0.24	0.56	0.02
Sr	8.06	15	7.1	18.09	7.5	7.77	9.99	7.7
Rb	0.38	5	2.56	6.11	0.16-0.2	0.15	2.3	0.11
Li	0.40	4	7.68	5.92	0.4-0.6	1.21	2.72	0.19
K	-	-	958	1584	-	438	1056	0.38
Mg	1201	0	0	0	1200	1271	682	1265
Mn	1.52	30	46.7	10.1	1.0-3.1	0.37	7.09	<0.001
Fe ppb	0.15	3	88800	5500	12	2.5	709	<0.001
Cu	-	-	1400	<0.06	-	3.4	0.1	<0.001
Zn	-	-	4800	1310	-	30	22	<0.001
Ag	-	-	2.1	12.4	-	-	-	-
Pb	-	-	56.2	67.5	-	-	-	-
As	-	-	18.1	50.8	-	-	-	-

1) measured vent fluid at 29°C (CASM II 1985) and calculated end-member concentrations at 350°C (this study). 2) average end-member concentrations for 4 vents (Edmond et al. 1982, Von Damm 1983). 3) average end-member concentrations for 10 vents (Von Damm 1983).4) measured vent fluids from Edmond et al. (1979a,b). 5) average 4 measured vent fluids at 25-85°C and 2 vent fluids at 276°C and 306°C from Tunnicliffe et al. (1986). 6) from Von Damm (1983). 7) saturated with respect to calcium carbonate. -) not determined.

count for the calculated concentration of 1139 ppm SiO_2 in the end-member (Fournier 1983). Vent fluids at <350°C are supersaturated with respect to quartz, but amorphous silica is the only phase found in the deposit, suggesting that the kinetics of precipitation are an important variable. The temperature of amorphous silica precipitation at Axial Seamount can be estimated from published solubility data (Fig. 17). In a vent fluid with seawater salinity (0.5 molal NaCl) and 1139 ppm SiO_2 at 150 bars (1500 m depth), the maximum temperature of amorphous silica saturation is 235°C (Fig. 17). Precipitation of amorphous silica at this temperature requires direct conductive cooling of the end-member fluid from 350°C. However, because of the low temperature of barite-silica mineralization (*e.g.*, 185°C) and the variations in Sr/Ba ratios in associated barite, we favor a combination of conductive cooling and mixing with ambient seawater at or near the site of deposition to account for amorphous silica precipitation. For example, the coprecipitation of amorphous silica and barite at 185°C, during the early barite-silica stage, could have resulted from initial conductive cooling from 350°C to about 275°C, followed by mixing to a solution containing nearly 50 wt.% seawater (Fig. 17).

Sulfur Isotopes

Sulfur isotope ratios were determined for a suite of sulfides and sulfates through the spire. The sulfur isotope compositions of FeS_2 (marcasite and pyrite), ZnS (sphalerite and wurtzite), and $BaSO_4$ relative to Cañon Diablo troilite (CDT) are reported in Table 3.

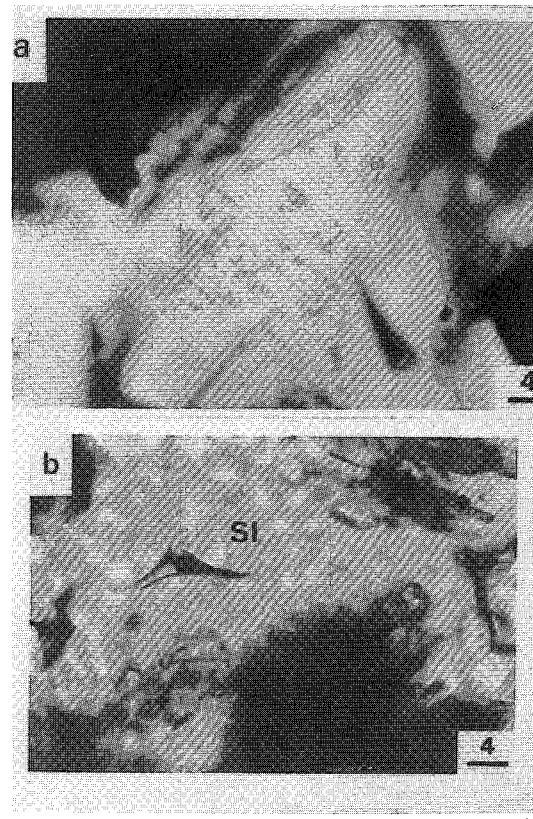

FIG. 15. a) Primary, two-phase fluid inclusions in wurtzite. b) Two-phase fluid inclusions in amorphous silica. Scale bars are in micrometers.

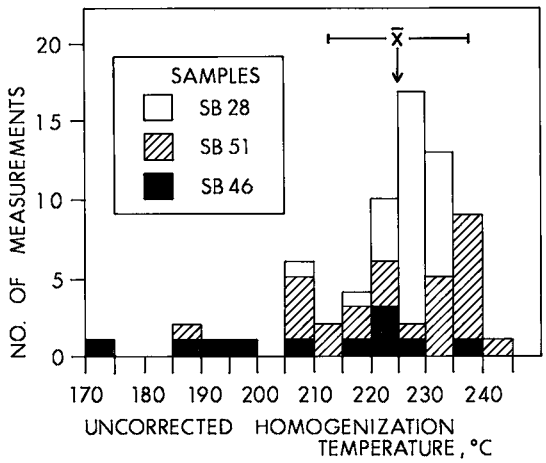

FIG. 16. Uncorrected homogenization temperatures for 67 primary and pseudosecondary fluid inclusions in wurtzite from three samples of the Axial Seamount spire. The mean, uncorrected homogenization temperature is 225°C ± 13°C (s.d.).

Isotopic disequilibrium between FeS_2 and ZnS is indicated by reversed enrichment factors. Under equilibrium conditions, FeS_2 should have a higher $\delta^{34}S$ than ZnS (Ohmoto 1972, Ohmoto & Rye 1979). Sulfide–sulfate disequilibrium is indicated by the unreasonable temperatures that are calculated if isotopic equilibrium between mineral pairs is assumed: 412°C for FeS_2–$BaSO_4$, and 449°C for ZnS–$BaSO_4$ based on fractionation factors from Ohmoto (1972). Similar isotopic disequilibrium has been identified in most seafloor sulfide deposits investigated (*e.g.*, 21°N: Arnold & Sheppard 1981, Styrt *et al.* 1981, Kerridge *et al.* 1983, Zierenberg *et al.* 1984, Woodruff & Shanks 1987; Guaymas Basin: Koski *et al.* 1985, Shanks & Niemitz 1982, Peter 1986; Red Sea: Shanks & Bischoff 1977, 1980).

The average $\delta^{34}S$ of sulfides from Axial Seamount (4.0 per mil) is higher than that of sulfides from high-temperature vents at 21°N (≤2 per mil: Styrt *et al.* 1981, Kerridge *et al.* 1983, Zierenberg *et al.* 1984, Woodruff & Shanks, 1988), and resembles the $\delta^{34}S$ of sulfides from the Galapagos mounds (5 to 6 per mil: Skirrow & Coleman 1982) and 13°N (4 per mil: Bluth & Ohmoto 1986). Bluth & Ohmoto (1986) suggested that variations in the $\delta^{34}S$ of H_2S in the vent fluids may be a result of changing water–rock reactions at depth during the evolution of a hydrothermal system. However, Shanks & Janecky (1984), Woodruff & Shanks (1988) and Shanks & Seyfried (1987) have shown that reduction of seawater sulfate during local, nonequilibrium mixing is a principal cause of increasing $\delta^{34}S$ values in sulfide chimneys at 21°N and the southern Juan de Fuca Ridge. Mixing of H_2S-rich vent fluid with SO_4-rich seawater at 200–300°C would result in the simultaneous reduction of SO_4 by ferrous Fe in the hydrothermal fluid, and oxidation of H_2S (Ohmoto & Rye 1979). This mixing of isotopically heavy, seawater sulfate with light, reduced sulfur from the vent fluids at or near the site of deposition is likely to obscure the importance of a deep-seated source of sulfur. If sulfur in the spire from Axial Seamount is derived from such a mixture, the 1–2 per mil difference in the $\delta^{34}S$ of the sulfides relative to the $\delta^{34}S$ of H_2S in a typical end-member fluid (*e.g.*, 2.1 per mil at 21°N: Woodruff & Shanks 1988) would require the reduction of about 5–10 mole% SO_4 from seawater (21 per mil: Rees *et al.* 1978). Most of the barite in the spire has the isotopic composition of

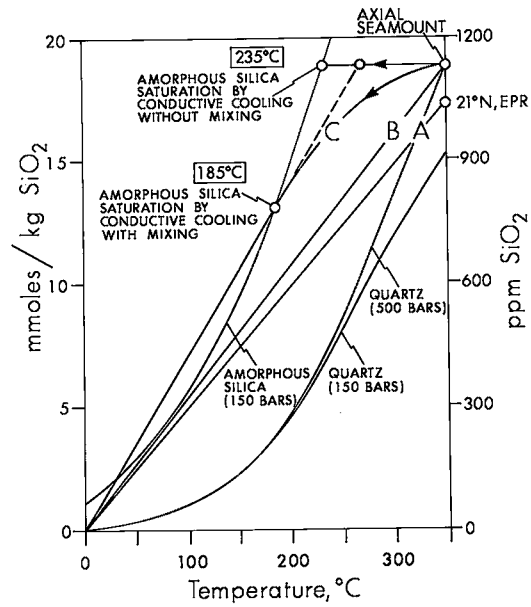

FIG. 17. Solubility of amorphous silica and quartz showing possible cooling curves preceding the deposition of amorphous silica at Axial Seamount (18.9 mmoles/kg SiO_2 end-member concentration) and 21°N, EPR (17.6 mmoles/kg SiO_2 end-member concentration). A minimum temperature of 350°C is required to account for 18.9 mmoles/kg SiO_2 in the Axial Seamount end-member in equilibrium with quartz at depth (*e.g.*, 500 bars). Amorphous silica saturation at 150 bars would occur at 235°C by conductive cooling without mixing. Simple mixing without conductive cooling cannot account for amorphous silica deposition from end-member fluids at either 21°N (mixing line A: Janecky & Seyfried 1984) or Axial Seamount (mixing line B: this study). A combination of conductive cooling and simple mixing (C) allows for amorphous silica saturation at Axial Seamount at temperatures below 235°C. Solubility data for quartz and amorphous silica are from Fournier (1983) and Chen & Marshall (1982), respectively.

TABLE 3. SULFUR ISOTOPE COMPOSITION (PER MIL) OF SULFIDES AND SULFATE FROM THE AXIAL SEAMOUNT SPIRE

Samples from the Recovered Spire:				
Section	Sample	FeS_2	ZnS	$BaSO_4$
Exterior[1]	SB33	3.8	4.9	-
	SB20	3.9	5.7	-
	SB20d[2]	3.2	4.9	-
Basal	SB15	3.3	4.9	16.3
Section	SB15d	3.2	5.0	-
	SB22	3.5	4.7	-
	SB30	3.7	4.3	-
	SB30d	4.0	3.7	-
	S49	2.4	4.8	-
	S49d	2.8	5.5	-
	S54	3.1	5.0	20.9
Upper	S55	-	4.7	-
Section	S57	-	5.0	-
	S53	2.8	-	21.2
	S56	3.5	5.5	-
Average[3]		3.3 ± 0.5	4.9 ± 0.5	19.5 ± 2.7
Interior	I	-	4.7	16.9
	SB13	3.5	4.2	-
	SB44	2.9	4.5	-
Basal	SB41	2.0	4.7	20.4
Section	SB32	3.1	4.4	20.8
	SB46	1.1	4.3	16.0
	SB26	3.5	4.7	-
	SC52	3.2	4.2	20.1
Central	SC52d	3.7	4.7	-
Section	SC50	2.9	4.6	-
	SC51	3.8	4.3	-
Average		3.0 ± 0.8	4.5 ± 0.2	18.8 ± 2.2
Other Samples:				
	1324-2 (1)	3.2	5.2	21.0
	1324-2 (5)	3.5	2.3	-
	1324-2 (6)	3.6	4.8	19.7
	1324-2 (7)	3.8	5.1	-
Other Spires:				
	1327-2	4.6	5.3	22.1
	1323	2.9	5.2	21.3
	1326	-	-	21.5

1) samples from the exterior of the spire or from fossil sulfate-rich walls within the spire. 2) d = duplicate sample. 3) averages quoted ± one standard deviation.

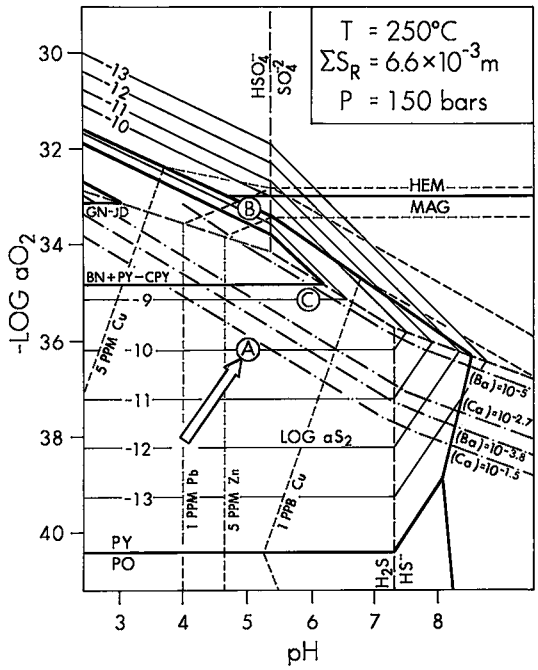

FIG. 18. Estimated log aO_2–pH for sulfide deposition at Axial Seamount (A) deduced from geochemical constraints discussed in the text. Principal aqueous sulfur species (long dashes) are calculated from Helgeson (1969). Stability fields for pyrite (PY), pyrrhotite (PO), magnetite (MAG), and hematite (HEM) (bold lines) and aS_2 contours (fine lines) are from Helgeson (1969), Robie *et al.* (1978), and Toulmin & Barton (1964). Limits of barite solubility at concentrations of $10^{-4.6}$ *m* Ba^{+2} (end-member fluid) and $10^{-3.8}$ *m* Ba^{+2} (solubility at 250°C, 0.5 *m* NaCl, and pH 5: Blount 1977) and anhydrite solubility at $10^{-1.5}$ *m* Ca^{+2} (end-member fluid) and $10^{-2.7}$ *m* Ca^{+2} (solubility at 250°C and 0.5 *m* NaCl: Blount & Dickson 1969) are shown as dash-dot lines. Selected solubility contours for the major sulfides (short dashes) are derived from Barrett & Anderson (1982) and Crerar & Barnes (1976) for 0.5 *m* NaCl. The sulfidation boundary for chalcopyrite – pyrite + bornite (CPY–PY + BN) is determined from Helgeson (1969) and Schneeberg (1973); galena – jordanite (GN–JD) is calculated from Craig & Barton (1973) assuming 100 ppb As in solution. Fluids at Axial Seamount (A) may be derived from higher-temperature fluids at a lower pH and aO_2 (schematic arrow). Conditions of mineralization for black ore in the Kuroko deposits resemble those at Axial Seamount and also plot at (A) (Ohmoto *et al.* 1983, Pisutha-Arnond & Ohmoto 1983); black siliceous ore and yellow siliceous ore from a typical Kuroko deposit plot at (B) and (C) respectively (Bryndzia *et al.* 1983).

contemporaneous seawater, but $\delta^{34}S$ values as low as +16 to +18 per mil could also be accounted for by mixing and the incorporation of light sulfur from oxidized H_2S.

Isotopic mixing in some chimneys may also occur as a result of replacement of sulfates by sulfides. Although replacement of anhydrite may be common in black-smoker chimneys, the barite in the Axial Seamount spire is isolated from the main-stage sulfides by amorphous silica. Therefore, heavy sulfur in the sulfides from Axial Seamount is not likely to have been derived from replacement of pre-existing barite.

Conditions of Deposition

The physical and chemical conditions of mineralization for the Axial Seamount spire can be estimated from mineral equilibria pertinent to the observed assemblages at 250°C, together with the extrapolated composition of the end-member fluid. Mineral equilibria are useful for comparing conditions of mineralization, but must be considered with caution because of the widespread disequilibrium during sulfide deposition on the seafloor. Thermodynamic calculations for the main stage of mineralization in the Axial Seamount spire are made at

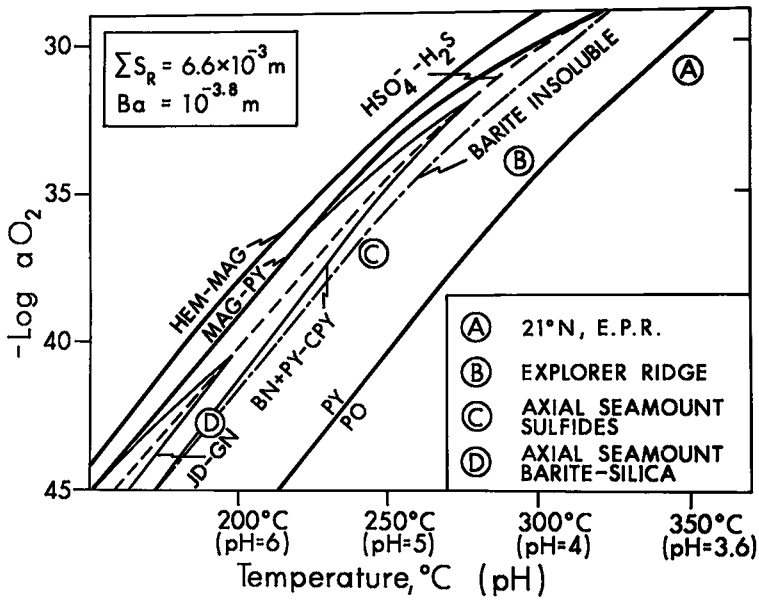

FIG. 19. Estimated log aO_2–temperature–pH conditions of mineralization at different seafloor polymetallic sulfide deposits. Principal aqueous sulfur species, stability fields for iron oxides and sulfides, sulfidation reactions, and the solubility limit for barite at $10^{-3.8}$ *m* Ba^{+2} are calculated as for Figure 18. The pH is assumed to vary with temperature according to the mixing model of Janecky & Seyfried (1984). Estimated conditions of mineralization at Axial Seamount are plotted at 235°C (sulfide stage) and 185°C (barite–silica stage). Mature hydrothermal deposits at Axial Seamount and Southern Explorer Ridge could have evolved from high-temperature fluids like those at 21°N along a hypothetical cooling-mixing path (A to D).

the maximum, corrected, fluid-inclusion temperature of 250°C and a total reduced sulfur content (ΣS_R) of 6.6 × 10^{-3} molal, corresponding to the extrapolated 224 ppm H_2S in the calculated end-member fluid (Table 2).

Although marcasite is the dominant Fe sulfide in the spire, we assume that the hydrothermal fluid was in equilibrium with pyrite. Marcasite is known to be metastable with respect to pyrite at 250°C and pH = 5 (Rising 1973, Craig & Scott 1982, Murowchick & Barnes 1986) and is not abundant in higher temperature (>300°C) chimneys on the seafloor. Wurtzite is stable in equilibrium with pyrite only at low temperatures and low sulfur activity (Scott & Barnes 1972), but is found primarily in the cores of recently active chimneys or spires and not in the lower temperature sulfides. In general, wurtzite seems to be stable relative to sphalerite under conditions of active venting but becomes unstable when venting ceases.

The activity of sulfur in equilibrium with pyrite is determined from the FeS content of coexisting sphalerite at a known temperature (Barton & Toulmin 1966, Czamanske 1974, Scott 1983). At 250°C the FeS content of sphalerite in the Axial Seamount spire (0.1 to 6 mole % FeS: Fig. 12) indicates a range in activity of sulfur from $10^{-8.3}$ to $10^{-11.8}$ or a mean near 10^{-10}.

The conditions of sulfide mineralization at Axial Seamount (*i.e.*, 250°C, pH = 5, log aS_2 = –10) can be demonstrated on a log aO_2–pH diagram (Fig. 18). As neither barite nor anhydrite was present during main-stage sulfide mineralization, the Axial Seamount fluid is constrained to a pH and aO_2 below the solubility limits for these minerals at 250°C. Chalcopyrite was stable with respect to bornite in fluids at 250°C, but later fluids that altered galena to jordanite must have been cooler (<200°C) and relatively more oxidizing. The conditions of sulfide formation at Axial Seamount are similar to those of the Kuroko deposits (Fig. 18) and likely reflect a similar origin. The mineralogy and geochemistry of typical black ore from Kuroko deposits are virtually identical to those of the Axial Seamount spire and are plotted at the same pH and aO_2 on Figure 18.

The hydrothermal fluid that precipitated sulfides at Axial Seamount evidently evolved from a reducing fluid at a low pH and high temperature (350°C),

similar to that at 21°N, to a relatively oxidizing fluid at a higher pH and lower temperature by conductive cooling and mixing with seawater. This difference is illustrated by comparing the conditions of mineralization at Axial Seamount, Southern Explorer Ridge, and 21°N (Table 4) on a log aO_2–temperature–pH diagram (Fig. 19). The fluids from these deposits can be interpreted as lying along a hypothetical cooling–mixing path (A to D on Fig. 19) similar to that calculated by Janecky & Seyfried (1984). The mineralogical zonation produced by the evolution of a vent fluid along this path (*e.g.*, high-temperature pyrrhotite-rich assemblages followed by lower-temperature pyrite–chalcopyrite–bornite assemblages and late-stage barite) is similar to that found in ancient massive sulfide deposits (*e.g.*, Large 1977). Furthermore, the range of conditions represented by A to D on Figure 19 can also be expected to occur within individual chimneys, leading to significant mineralogical variations at a much smaller scale.

TABLE 4. ESTIMATED CONDITIONS OF SULFIDE DEPOSITION AT SELECTED SEAFLOOR POLYMETALLIC SULFIDE DEPOSITS

	Axial[1] Seamount	21°N[2] EPR	Explorer[3] Ridge	Southern Juan[4] de Fuca Ridge	Endeavour[5] Ridge
pH	5	3.6	4.6-5.0	3.2	
T °C	235-250	355	276-306	224-284	100-405
mole % FeS in sphal.	0.1-6	3-37	1-22	2-18	20-40
	(72)	(42)	(250)	(75)	(16)
log aS_2[7]	-8.3 to -11.8	-7.0 to -12.5	-8.5 to -11.5	-10.5 to -12.7	-9.0 to -14.0
log aO_2	-36	-31	-34	-38	<-31
iron	PY	PY ± PO	PY	PY ± PO	PY ± PO

1) this study. 2) Arnold & Sheppard (1981), Haymon & Kastner (1981), Haymon (1983), Von Damm (1983), Zierenberg et al. (1984). 3) Hannington (1986), Tunnicliffe et al. (1986), Hannington & Scott (1987). 4) Koski et al. (1984), U.S.G.S. Juan de Fuca Study Group (1986). 5) Kingston et al. (1983), MERGE Group (1984), Tivey & Delaney (1986). 6) mole % FeS in sphalerite from published microprobe anlyses (brackets refer to numbers of anlyses). 7) estimated activities of sulfur and oxygen at the specified temperatures and ΣS_x =250 ppm H_2S, based on the FeS content of sphalerite in equilibrium with the major iron sulfides (PY pyrite, PO pyrrhotite).

Conclusions

The growth of large sulfide-bearing structures is important for the efficient accumulation of sulfides in a number of deposits on the seafloor and may have been important in ancient volcanogenic massive sulfide deposits now found on land. In the northern vent-field at Axial Seamount, these large spires resemble the late-stage, low-temperature (<300°C) caps on other mature seafloor sulfide deposits. Growth of the spires is made possible by the precipitation of abundant spire-constructing silica and barite, and is facilitated by a biological substrate. Mineral paragenesis and growth are related to temperature and the degree of mixing between hydrothermal fluids and seawater as indicated by silica geothermometry, fluid inclusions, Sr/Ba ratios in barite, and sulfur isotopes. Substantial cooling is required for the deposition of amorphous silica and barite, and may be necessary in order to form the large sulfide-bearing structures on top of mature deposits. A comparison of the temperature-pH-aS_2-aO_2 conditions for different deposits indicates that the vent fluids responsible for the growth of large spires at Axial Seamount may have been derived from higher temperature 21°N-type fluids, by a combination of conductive cooling and mixing. Local mixing of high-temperature fluids with seawater near the surface of the deposits accounts for the growth of large, low-temperature spires accompanying high-temperature mineralization at the same site.

Acknowledgements

Samples and geological observations used in this study were obtained during the 1983 CASM I (R.L. Chase, Chief Scientist) and II (V. Tunnicliffe, Chief Scientist) cruises with the PISCES IV submersible and support vessel MV *PANDORA II*. We thank Fisheries and Oceans Canada, and Energy, Mines and Resources Canada, for their support. E.T.C. Spooner helped with the study of fluid inclusions. Sulfur isotope analyses were provided by I.R. Jonasson and G.E.M. Hall (Geological Survey of Canada) and by W.C. Shanks and L.G. Woodruff (U.S.G.S., Reston). R. G.V. Hancock (Slowpoke Reactor Facility, University of Toronto) helped with neutron-activation analyses. G. Taylor prepared polished thin sections. S. Shanbag and B. O'Donovan drafted and photographed the Figures. E. Ambrose helped prepare the manuscript. Our work at Axial Seamount has benefitted from discussion with R.L. Chase, J.R. Delaney, H.P. Johnson, J.L. Karsten, E.T.C. Spooner, G.M. Anderson, J.M. Peter, and T.F. McConachy. Two reviewers for *The Canadian Mineralogist* are thanked for their helpful comments and suggestions. Funding for this research was provided by NSERC Grants A7069, A5939, and G1111 to S.D. Scott.

References

Arnold, M. & Sheppard, S.M.F. (1981): East Pacific Rise at latitude 21°N: isotopic composition and origin of the hydrothermal sulfur. *Earth Planet. Sci. Lett.* **56**, 148-156.

ASHES Expedition (1986): Pisces submersible exploration of a high-temperature vent field in the caldera of Axial Seamount, Juan de Fuca Ridge. *EOS, Trans. Amer. Geophys. Union* **67**, 1027.

Barrett, T.J. & Anderson, G.M. (1982): The solubility of sphalerite and galena. *Econ. Geol.* **77**, 1923-1933.

BARTON, P.B., JR. & TOULMIN, P., III (1966): Phase relations in the Fe–Zn–S system. *Econ. Geol.* **61**, 815-849.

BATIZA, R. (1982): Lithospheric age dependence of off-ridge volcano production in the North Pacific. *Geophys. Res. Lett.* **8**, 853-856.

BISCHOFF, J.L. & SEYFRIED, W.E. (1978): Hydrothermal chemistry of seawater from 25°–350°C. *Amer. J. Sci.* **278**, 838-860.

BLOUNT, C.W. (1977): Barite solubilities and thermodynamic properties up to 300°C and 1400 bars. *Amer. Mineral.* **62**, 942-957.

_____ & DICKSON, F.W. (1969): The solubility of anhydrite ($CaSO_4$) in NaCl–H_2O from 100 to 450°C and 1 to 1000 bars. *Geochim. Cosmochim. Acta* **33**, 227-245.

BLUTH, G. & OHMOTO, H. (1986): Sulfur isotope geochemistry of vent sites from the East Pacific Rise at 13°N. *Geol. Soc. Amer. Program Abstr.* **18**, 544.

BOWERS, T.S., VON DAMM, K.L. & EDMOND, J.M. (1985): Chemical evolution of ridge-crest hot springs. *Geochim. Cosmochim. Acta* **49**, 2239-2252.

BRYNDZIA, L.T., SCOTT, S.D. & FARR, J.E. (1983): Mineralogy, geochemistry, and mineral chemistry of siliceous ore and related footwall rocks in the Uwamuki 2 and 4 deposits, Kosaka Mine, Hokuroku District, Japan. *Econ. Geol. Monogr.* **5**, 507-522.

CASM II (1985): Hydrothermal vents on an axis seamount of the Juan de Fuca Ridge. *Nature* **313**, 212-214.

CASM III (1985): Exploration of Southern Explorer Ridge for hydrothermal vent fields. *EOS, Trans. Amer. Geophys. Union* **66**, 23.

CATHLES, L.M. (1983): An analysis of the hydrothermal system responsible for massive sulfide deposition in the Hokuroku basin of Japan. *Econ. Geol. Monogr.* **5**, 439-487.

CHEN, C.T.A. & MARSHALL, W.L. (1982): Amorphous silica solubilities IV. Behaviour in pure water and aqueous sodium chloride, sodium sulfate, magnesium chloride, and magnesium sulfate solutions up to 350°C. *Geochim. Cosmochim. Acta* **46**, 279-287.

CONVERSE, D.R., HOLLAND, H.D. & EDMOND, J.M. (1984): Flow rates in the axial hot springs of the East Pacific Rise (21°N). *Earth Planet. Sci. Lett.* **69**, 159-175.

COUSENS, B.L., CHASE, R.L. & SCHILLING, J.-G. (1984): Basalt geochemistry of the Explorer Ridge area, northeast Pacific Ocean. *Can. J. Earth Sci.* **21**, 157-170.

CRAIG, J.R. & BARTON, P.B., JR. (1973): Thermochemical approximations for sulfosalts. *Econ. Geol.* **68**, 493-506.

_____ & SCOTT, S.D. (1982): Sulfide phase equilibia. *In* Sulfide Mineralogy (P.H. Ribbe, ed.). Mineral. Soc. Amer., Rev. Mineral. **1**, CS1-110.

CRANE, K., AIKMAN, F., EMBLEY, R., HAMMOND, S., MALAHOFF, A. & LUPTON, J. (1984): The distribution of geothermal fields on the Juan de Fuca Ridge. *J. Geophys. Res.* **90**, 727-744.

CRERAR, D.A. & BARNES, H.L. (1976): Ore solution chemistry V. Solubilities of chalcopyrite and chalcocite assemblages in hydrothermal solutions at 200 to 350°C. *Econ. Geol.* **71**, 772-794.

CZAMANSKE, G.K. (1974): The FeS content of sphalerite along the chalcopyrite–pyrite–bornite sulfur fugacity buffer. *Econ. Geol.* **69**, 459-461.

EDMOND, J.M., MEASURES, C., MANGUM, B., GRANT, B., SCLATTER, F.R., COLLIER, R., HUDSON, A., GORDON, L.I. & CORLISS, J.B. (1979a): On the formation of metal-rich deposits at ridge crests. *Earth Planet. Sci. Lett.* **46**, 19-30.

_____, _____, MCDUFF, R.E., CHAN, L.H., COLLIER, R. & GRANT, B. (1979b): Ridge crest hydrothermal activity and balances of the major and minor elements in the ocean: the Galapagos data. *Earth Planet. Sci. Lett.* **46**, 1-18.

_____, VON DAMM, K.L., MCDUFF, R.E. & MEASURES, C.I. (1982): Chemistry of hot springs on the East Pacific Rise and their effluent dispersal. *Nature* **297**, 187-191.

ELDRIDGE, C.S., BARTON, P.B., JR. & OHMOTO, H. (1983): Mineral textures and their bearing on formation of the Kuroko orebodies. *Econ. Geol. Monogr.* **5**, 241-281.

FARRELL, C.W. (1979): *Strontium Isotopes of Kuroko Deposits.* Ph.D. thesis, Harvard Univ., Cambridge, Mass.

_____ & HOLLAND, H.D. (1983): Strontium isotope geochemistry of the Kuroko deposits. *Econ. Geol. Mono.* **5**, 302-319.

FOURNIER, R.O. (1983): A method of calculating quartz solubilities in aqueous sodium chloride solutions. *Geochim. Cosmochim. Acta* **47**, 579-586.

GOLDFARB, M.S., CONVERSE, D.R., HOLLAND, H.D. & EDMOND, J.M. (1983): The genesis of hot spring deposits on the East Pacific Rise, 21°N. *Econ. Geol. Monogr.* **5**, 184-197.

HANNINGTON, M.D. (1986): *Geology, Mineralogy, and Geochemistry of a Silica–Sulfate–Sulfide Deposit, Axial Seamount, N.E. Pacific Ocean.* M.Sc. thesis, Univ. of Toronto, Toronto, Ontario.

_____, PETER, J.M. & SCOTT, S.D. (1986): Gold in sea-floor polymetallic sulfide deposits. *Econ. Geol.* **81**, 1867-1883.

_____ & SCOTT, S.D. (1987): Sulfidation equilibria as guides to gold mineralization in volcanogenic massive sulfides. *Geol. Soc. Amer. Program Abstr.* **19**, 692.

HAYMON, R.M. (1983): Growth history of hydrothermal black smoker chimneys. *Nature* **305**, 695-698.

_____ & KASTNER, M. (1981): Hot spring deposits on the East Pacific Rise at 21°N: preliminary description of mineralogy and genesis. *Earth Planet. Sci. Lett.* **53**, 363-381.

_____, KOSKI, R.A. & SINCLAIR, C. (1984): Fossils of hydrothermal vent worms from Cretaceous sulfide ores of the Semail Ophiolite, Oman. *Science* **223**, 1407-1409.

HÉKINIAN, R., FEVRIER, M., BISCHOFF, J.L., PICOT, P. & SHANKS, W.C. (1980): Sulfide deposits from the East Pacific Rise near 21°N. *Science* **207**, 1433-1444.

_____ & FOUQUET, Y. (1985): Volcanism and metallogenesis of axial and off-axial structures on the East Pacific Rise near 13°N. *Econ. Geol.* **80**, 221-249.

_____, FRANCHETEAU, J. & BALLARD, R.D. (1985): Morphology and evolution of hydrothermal deposits at the axis of the East Pacific Rise. *Oceanol. Acta* **8**, 147-155.

HELGESON, H.C. (1969): Thermodynamics of hydrothermal systems at elevated temperatures and pressures. *Amer. J. Sci.* **267**, 729-804.

JANECKY, D.R. & SEYFRIED, W.E., JR. (1984): Formation of massive sulfide deposits on oceanic ridges: Incremental reaction models for mixing between hydrothermal solutions and seawater. *Geochim. Cosmochim. Acta* **48**, 2723-2738.

JOHNSON, H.P. & TUNNICLIFFE, V. (1985): Time-series measurements of hydrothermal activity on the northern Juan de Fuca Ridge. *Geophys. Res. Lett.* **12**, 685-688.

_____ & _____ (1986): Time-lapse camera measurements of a high-temperature hydrothermal system on Axial Seamount: Juan de Fuca Ridge. *EOS, Trans. Amer. Geophys. Union* **67**, 1283.

JONES, J.B. & SEGNIT, E.R. (1971): The nature of opal. Nomenclature and constituent phases. *J. Geol. Soc. Australia* **18**, 56-78.

JUNIPER, S.K. & FOUQUET, Y. (1988): Filamentous iron-silica deposits from modern and ancient hydrothermal sites. Can. Mineral. **26**, 859-869.

KAJIWARA, Y. (1973): Chemical composition of ore-forming solutions responsible for Kuroko type mineralization in Japan. *Geochem. J. (Japan)* **6**, 141-149.

KALOGEROPOULOS. S.I. & SCOTT, S.D. (1983): Mineralogy and geochemistry of tuffaceous exhalites (Tetsusekiei) of the Fukazawa Mine, Hokuroku District, Japan. *Econ. Geol. Monogr.* **5**, 412-432.

_____ & _____ (1986): On the genesis of barite associated with volcanogenic massive sulfides, Fukazawa Mine, Hokuroku District, Japan. *In* Geology and Metallogeny of Copper Deposits (G.H. Friedrich, A.D. Genkin, A.J. Naldrett, J.D. Ridge, R.H. Sillitoe & F.M. Vokes, eds.). Springer-Verlag, Berlin, 371-388.

KANO, K. & TAGUCHI, K. (1982): Experimental study on the ordering of opal-CT. *Geochem. J. (Japan)* **16**, 33-41.

KERRIDGE, J.F., HAYMON, R.M. & KASTNER, M. (1983): Sulfur isotope systematics at the 21°N site, East Pacific Rise. *Earth Planet. Sci. Lett.* **66**, 91-100.

KINGSTON, M.J., DELANEY, J.R. & JOHNSON, H.P. (1983): Sulfide deposits from the Juan de Fuca Ridge at 45°57'N, 129°06'W. *Proc. Oceans '83 Volume II, San Francisco*, 811-815.

KOSKI, R.A., CLAGUE, D.A. & OUDIN, E. (1984): Mineralogy and chemistry of massive sulfide deposits from the Juan de Fuca Ridge. *Geol. Soc. Amer. Bull.* **95**, 930-945.

_____, LONSDALE, P.F., SHANKS, W.C., BERNDT, M.E. & HOWE, S.S. (1985): Mineralogy and geochemistry of sediment-hosted hydrothermal sulfide deposits from the Southern Trough of Guaymas Basin, Gulf of California. *J. Geophys. Res.* **90**, 6695-6707.

LARGE, R. (1977): Chemical evolution and zonation of massive sulfide deposits in volanic terrains. *Econ. Geol.* **72**, 549-572.

MACDONALD, A.J. & SPOONER, E.T.C. (1981): Calibration of a Linkham TH600 programmable heating-cooling stage for microthermometric examination of fluid inclusions. *Econ. Geol.* **76**, 1248-1258.

MACDONALD, K.C., BECKER, K., SPIESS, F.N. & BALLARD, R.D. (1980): Hydrothermal heat flux of the "black smoker" vents of the East Pacific Rise. *Earth Planet. Sci. Lett.* **48**, 1-7.

MALAHOFF, A., MCMURTRY, G., HAMMOND, S. & EMBLEY, R. (1984): High temperature hydrothermal fields – Juan de Fuca Ridge axial volcano. *EOS, Trans. Amer. Geophys. Union* **65**, 1112.

MCDUFF, R.E., EDMOND, J.M., JUNIPER, K., LUPTON, J.E. & SCOTT, S.D. (1983): The chemistry of hydrothermal water, Axial Seamount, Juan de Fuca Ridge. *EOS, Trans. Amer. Geophys. Union* **64**, 723.

MERGE (1984): Regional setting and character of a

hydrothermal field/sulfide deposit on the Endeavour Segment of the Juan de Fuca Ridge. *EOS, Trans. Amer. Geophys. Union* **65**, 1111.

MUROWCHICK, J.B. & BARNES, H.L. (1986): Marcasite precipitation from hydrothermal solutions. *Geochim. Cosmochim. Acta* **50**, 2615-2629.

OHMOTO, H. (1972): Systematics of sulfur and carbon isotopes in hydrothermal ore deposits. *Econ. Geol.* **67**, 551-578.

_____ (1978): Submarine calderas: a key to the formation of volcanogenic massive sulfide deposits? *Mining Geol.* **28**, 219-231.

_____, MIZUKAMI, M., DRUMMOND, S.E., ELDRIDGE, C.S., PISUTHA-ARNOND, V. & LENAGH, T.C. (1983): Chemical processes of Kuroko formation. *Econ. Geol. Monogr.* **5**, 570-604.

_____ & RYE, R.O. (1974): Hydrogen and oxygen isotopic compositions of fluid inclusions in the Kuroko deposits, Japan. *Econ. Geol.* **69**, 947-953.

_____ & _____ (1979): Isotopes of sulfur and carbon. *In* Geochemistry of Hydrothermal Ore Deposits, 2nd ed. (H.L. Barnes, ed.). John Wiley & Sons, New York.

_____ & TAKAHASHI, T. (1983): Geologic setting of the Kuroko deposits, Japan. Part III. Submarine calderas and Kuroko genesis. *Econ. Geol. Monogr.* **5**, 39-54.

OUDIN, E. (1981): Études minéralogique et géochimique des dépôts sulfures sous-marins actuels de la ride Est-Pacifique (21°N). *Documents du Bureau Recherches Géologiques et Minières* **25**.

_____ (1983): Minéralogie de gisements et indices liés à des zones d'accrétion océaniques actuelles (ride Est Pacifique et Mer Rouge) et fossile (Cyphre). *Chronique Recherche Minière* **470**, 43-55.

_____ & CONSTANTINOU, G. (1984): Black smoker chimney fragments in Cyprus sulphide deposits. *Nature* **308**, 349-353.

PETER, J.M. (1986): *Geochemistry and Mineralogy of Hydrothermal Vent Precipitates from the Southern Trough of Guaymas Basin, Gulf of California.* M.Sc. thesis, Univ. of Toronto, Toronto, Ontario.

_____ & SCOTT, S.D. (1988): Mineralogy, composition and fluid-inclusion microthermometry of seafloor hydrothermal deposits in the southern trough of Guaymas Basin, Gulf of California. *Can. Mineral.* **26**, 567-587.

PICOT, P. & FEVRIER, M. (1980): Étude minéralogique d'échantillons du Golfe de Californie (Campagne Cyamex). *Documents du Bureau Recherches Géologiques et Minières* **20**.

PISUTHA-ARNOND, V. & OHMOTO, H. (1983): Thermal history, and chemical and isotopic compositions of the ore-forming fluids responsible for the Kuroko massive sulfide deposits in the Hokuroku District of Japan. *Econ. Geol. Monogr.* **5**, 523-558.

REES, C.E., JENKINS, W.J. & MONSTER, J. (1978): The sulfur isotopic composition of ocean water sulfate. *Geochim. Cosmochim. Acta* **42**, 377-382.

RISING, B.A. (1973): *Phase Relations Among Pyrite, Marcasite, and Pyrrhotite below 300°C.* Ph.D. thesis, Pennsylvania State Univ., University Park, Pennsylvania.

ROBIE, R.A., HEMINGWAY, B.S. & FISHER, J.R. (1978): Thermodynamic properties of minerals and related substances at 298.15 K and 1 bar pressure and at higher temperatures. *U.S. Geol. Surv. Bull.* **1452**.

RONA, P.A., KLINKHAMMER, G., NELSEN, T.A., TEFRY, J.H., & ELDERFIELD, H. (1986): Black smokers, massive sulfides, and vent biota at the Mid-Atlantic Ridge. *Nature* **321**, 33-37.

SATO, T. (1973): A chloride complex model for Kuroko mineralization. *Geochem. J. (Japan)* **7**, 245-270.

SCHISM I (1984): Along-strike variation in hydrothermal activity on Explorer Ridge, N.E. Pacific. *EOS, Trans. Amer. Geophys. Union* **65**, 1124.

SCHNEEBERG E.P. (1973): Sulfur fugacity measurements with the electrochemical cell $Ag/AgI/Ag_{2+x}S, fS_2$. *Econ. Geol.* **68**, 507-517.

SCOTT, S.D. (1978): Structural control of the Kuroko deposits of the Hokuroku District, Japan. *Mining Geol.* **28**, 301-311.

_____ (1980): Geology and structural control of Kuroko-type massive sulfide deposits. *In* The Continental Crust and Its Mineral Deposits (D.W. Strangway, ed.). *Geol. Assoc. Can. Spec. Pap.* **20**, 705-740.

_____ (1981): Small chimneys from Japanese Kuroko deposits. *In* Seminars on Sea-Floor Hydrothermal Systems (R. Goldie & T.J. Bottrill, eds.). *Geosci. Can.* **8**, 103-104.

_____ (1983): Chemical behaviour of sphalerite and arsenopyrite in hydrothermal and metamorphic environments. *Mineral. Mag.* **47**, 427-435.

_____ (1985): Seafloor polymetallic sulfide deposits: modern and ancient. *Mar. Mining* **5**, 191-212.

_____ & BARNES, H.L. (1972): Sphalerite–wurtzite equilibria and stoichiometry. *Geochim. Cosmochim. Acta* **36**, 1275-1295.

_____, CHASE, R.L., BARRETT, T.J., HANNINGTON, M., FOUQUET, Y. & JUNIPER, S.K. (1984): Tectonic

framework and sulfide deposits of Southern Explorer Ridge, Northeastern Pacific Ocean. *EOS, Trans. Amer. Geophys. Union* **65**, 1111.

_____, _____, MICHAEL, P.J., SHEA, G.T., BARRETT, T.J., GORTON, M., HANNINGTON, M. & PETER, J. (1985): Explorer Ridge and Tuzo Wilson Seamounts: update. *EOS, Trans. Amer. Geophys. Union* **66**, 925.

_____, _____ , HANNINGTON, M.D., MICHAEL, P.J., MCCONACHY, T.F. & SHEA, G.T. (1988): Sulfide deposits, tectonics, and petrogenesis of Southern Explorer Ridge, northeast Pacific Ocean. *Proc. Troodos '87, Ophiolite Symposium Volume* (in press).

SEYFRIED, W.E., JR. & BISCHOFF, J.L. (1981): Experimental seawater-basalt interaction at 300°C and 500 bars: Chemical exchange, secondary mineral formation, and implications for the transport of heavy metals. *Geochim. Cosmochim. Acta* **45**, 135-147.

_____ & MOTTL, M.J. (1982): Hydrothermal alteration of basalt by seawater under seawater-dominated conditions. *Geochim. Cosmochim. Acta* **46**, 985-1002.

SHANKS, W.C. & BISCHOFF, J.L. (1977): Ore transport and deposition in the Red Sea geothermal system: A geochemical model. *Geochim. Cosmochim. Acta* **41**, 1507-1519.

_____ & _____ (1980): Geochemistry, sulfur isotope composition, and accumulation rates of Red Sea geothermal deposits. *Econ. Geol.* **75**, 445-459.

_____ & JANECKY, D.R. (1984): Incremental reaction modelling and sulfur isotope evolution of seafloor hydrothermal fluids: 21°N and Juan de Fuca Rise. *Geol. Soc. Amer. Program Abstr.* **16**, 651.

_____, KOSKI, R.A. & WOODRUFF, L.G. (1984): Mineralogy and stable isotope systematics of sulfide deposits from the Juan de Fuca Ridge. *EOS, Trans. Amer. Geophys. Union* **65**, 1113.

_____ & NIEMITZ, J. (1982): 53. Sulfur isotope studies of hydrothermal anhydrite and pyrite, Deep Sea Drilling Project Leg 64, Guaymas Basin, Gulf of California. *Initial Reports of the Deep Sea Drilling Project* **64**(2), 1137-1142. U.S. Gov. Printing Office, Washington, D.C.

_____ & SEYFRIED, W.E., JR. (1987): Stable isotope studies of vent fluids and chimney minerals, Southern Juan de Fuca Ridge: Sodium metasomatism and seawater sulfate reduction. *J. Geophys. Res.* **92**, 387-399.

SHIKAZONO, N. & HOLLAND, H.D. (1983): The partitioning of strontium between anhydrite and aqueous solutions from 150° to 250°C. *Econ. Geol. Monogr.* **5**, 302-319.

SKIRROW, R. & COLEMAN, M.L. (1982): Origin of sulfur and geothermometry of hydrothermal sulfides from the Galapagos Rift, 86°W. *Nature* **299**, 142-144.

STARKE, R. (1962): Die Strontiumgehalte der Baryte. *Freiberg. Forschungsh.* **C**, 150.

STYRT, M.M., BRACKMANN, A.J., HOLLAND, H.D., CLARK, B.C., PISUTHA-ARNOND, V., ELDRIDGE, C.S. & OHMOTO, H. (1981): The mineralogy and isotopic composition of sulfur in hydrothermal sulfide/sulfate deposits on the East Pacific Rise, 21°N latitude. *Earth Planet. Sci. Lett.* **53**, 382-390.

TIVEY, M.K. & DELANEY, J.R. (1986): Growth of large sulfide structures on the Endeavor Segment of the Juan de Fuca Ridge. *Earth Planet. Sci. Lett.* **77**, 303-317.

TOULMIN, P., III & BARTON, P.B., JR. (1964): A thermodynamic study of pyrite and pyrrhotite. *Geochim. Cosmochim. Acta* **28**, 641-671.

TUNNICLIFFE, V., BOTROS, M., DE BURGH, M.E., DINET, A., JOHNSON, H.P., JUNIPER, S.K. & MCDUFF, R. (1986): Hydrothermal vents of Explorer Ridge, Northeast Pacific. *Deep-Sea Res.* **33**, 401-412.

URABE, T. (1974): Iron content of sphalerite coexisting with pyrite from some Kuroko deposits. *Soc. Mining Geol. Japan Special Issue* **6**, 377-384.

U.S.G.S. JUAN DE FUCA STUDY GROUP (1986): Submarine fissure eruptions and hydrothermal vents on the southern Juan de Fuca Ridge: Preliminary observations from the submersible Alvin. *Geology* **14**, 823-827.

VON DAMM, K.L. (1983): *Chemistry of Submarine Hydrothermal Solutions at 21°N, East Pacific Rise and Guaymas Basin, Gulf of California.* Ph.D. thesis, Mass. Inst. Tech./Woods Hole Oceanog. Inst., WHOI-84-3, Cambridge, Massachusetts.

_____, EDMOND, J.M., GRANT, B., MEASURES, C.I., WALDEN, B. & WEISS, R.F. (1985): Chemistry of submarine hydrothermal solutions at 21°N, East Pacific Rise. *Geochim. Cosmochim. Acta* **49**, 2197-2220.

WOODRUFF, L.G. & SHANKS, W.C., III (1988): Sulfur isotope study of chimney minerals and vent fluids from 21°N, East Pacific Rise: Hydrothermal sulfur sources and disequilibrium sulfate reduction. *J. Geophys. Res.* **93**, 4562-4572.

ZIERENBERG, R.A., SHANKS, W.C. & BISCHOFF, J.L. (1984): Massive sulfide deposits at 21°N, East Pacific Rise: Chemical composition, stable isotopes, and phase equilibria. *Geol. Soc. Amer. Bull.* **95**, 922-929.

Received February 5, 1987; revised manuscript accepted December 27, 1987.